2009

Green plastics, rubbers, coatings, and biocomposites from vegetable oils

Marlen Andrea Valverde
Iowa State University

Green plastics, rubbers, coatings, and biocomposites from vegetable oils

by

Marlen A. Valverde

A dissertation submitted to the graduate faculty

in partial fulfillment of the requirements for the degree of

DOCTOR OF PHILOSOPHY

Major: Organic Chemistry

Program of Study Committee:
Richard C. Larock, Major Professor
John Verkade
Klaus Schmidt-Rohr
Yan Zhao
Surya Mallapragada

Iowa State University

Ames, Iowa

2009

To my parents, Federico and Marlen, for giving me the thirst for knowledge and for teaching me the courage to achieve all of my goals, big and small.

A mis padres, Federico y Marlen, por darme la sed por el conocimiento y por ensenarme el coraje de obtener todas mis metas, grandes y pequenas.

TABLE OF CONTENTS

LIST OF ABBREVIATIONS

AIBN	2,2'-azobisisobutyronitrile
AN	acrylonitrile
BFE	boron trifluoride diethyl etherate
CLS	conjugated low saturation soybean oil
CNW	cellulose nanowhisker
CO	castor oil
CSOY	conjugated soybean oil
DCP	dicyclopentadiene
DMA	dynamic mechanical analysis
DMAc	*N*,*N*-dimethylacetamide
DMPA	dimethylolpropionic acid
DMF	*N*,*N*-dimethylformamide
DVB	divinylbenzene
EBE	ebecryl 860®
FT-IR	Fourier transform infrared spectroscopy
HDI	hexamethylenediisocyanate
HEX	1,5-hexadiene
ISO	isoprene
MCC	microcrystalline cellulose
MEK	methyl ethyl ketone
NMR	nuclear magnetic resonance

PU	polyurethane
RT	room temperature
SEM	scanning electron microscopy
SG	soy gold®
ST	styrene
TBPA	*tert*-butyl peracetate
TEA	triethylamine
TEM	transmission electron microspopy
TGA	thermogravimetric analysis
T_g	glass transition temperature
T_{max}	temperature of maximum degradation
T_{10}	temperature of 10% weight loss
T_{50}	temperature of 50% weight loss
wt %	weight percent
υe	crosslinking density
% insol	percent insoluble
% sol	percent soluble
E'	storage modulus
E"	loss modulus
E	Young's modulus

CHAPTER 1. GENERAL INTRODUCTION

The rapid growth of the world's population encourages the development of activities all linked to the usage of more materials that will make daily life easier and will increase efficiency; among these materials, plastics and rubbers are in the greatest demand.[1] Until very recently, these plastics and rubbers were synthesized almost exclusively from petroleum-based raw materials, which are linked with a series of environmentally harmful production processes, not to mention the fact that biological degradation of these materials is impossible, which creates an array of contamination issues. Recently, research scientists have joined the world's effort to minimize our dependence on petroleum by utilizing moderate amounts of bio-renewables in many materials that range from bio-compatible, tissue-like membranes to bio-fuels.[1,2] Choosing a viable "green" alternative to common petroleum-based starting materials is not an easy task, especially because the desired material has to have a high reactivity under many reaction conditions, it has to be cheap and readily available, and most importantly, once incorporated into a polymer, it has to show equal or better thermal and mechanical properties than the corresponding petroleum-based polymer. Carbohydrates, like cellulose or chitin,[3] and proteins, such as soy[4] or cheese protein,[5] have been extensively studied and incorporated into a large variety of materials. Unfortunately, the reaction conditions under which these materials can be used have to be very mild, limiting their possible usage.

Vegetable oils appear to be very attractive candidates for the preparation of bio-renewable materials for several reasons: (1) they are easily obtained from high-yielding crops; (2) there are a wide variety of vegetable oils, each one with a specific fatty acid

profile, which extends their range of applications; and (3) they can be successfully introduced into polymers as fast drying inks[5] and as a glue for wood materials,[6] although high molecular weight polymers have not been synthesized until recently.[7]

Vegetable oils consist of triglycerides differing in the number of carbon atoms present in the fatty acid chains, the number of carbon-carbon double bonds present, and the position of these double bonds within the chain.[8] In a few cases, vegetable oils also possess different functional groups.[9] The carbon-carbon double bonds make these oils suitable for polymerization, by processes such as cationic[10] or free radical polymerization,[11,12] and, if the double bonds are conjugated, thermal polymerization is also possible[13] (see Figure 1).

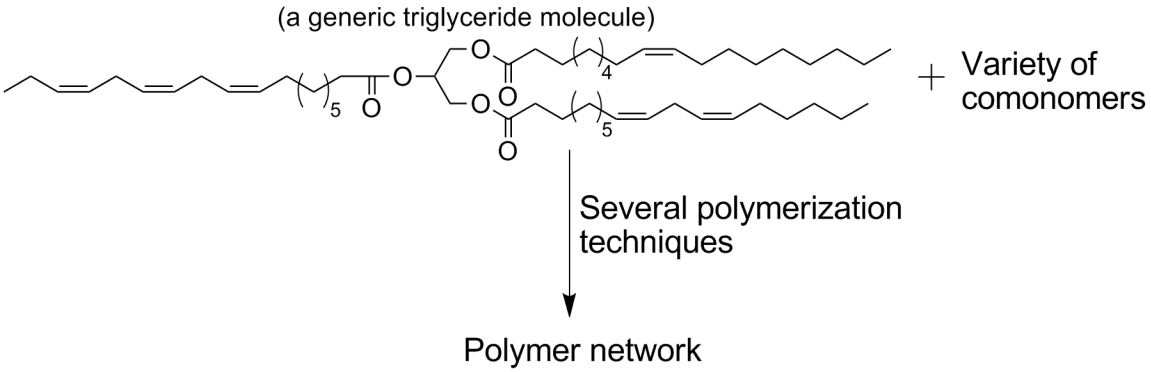

Figure 1. Generic polymerization reaction for a triglyceride molecule.

In Iowa, the two main crops are soybeans and corn. Both are very important in this new race towards a greener planet. These crops produce large quantities of vegetable oils possessing different fatty acid profiles.[14] Corn is mostly used industrially for the generation of ethanol, besides its primary food use. Soybeans are used for human food

and animal feed, and the remainder serves non-food uses (soaps, lubricants, and most importantly biodiesel).[15]

This relationship between Iowa's main crops and our research group's search for bio-renewable alternatives has produced a large number of research papers focused on the incorporation of vegetable oils into polymers that range from hard and brittle to soft and rubbery,[7-11] and lately even waterborne coatings.[16,17] Our search has not, however, been limited to corn and soybean oils, we have invested considerable time and effort in looking at other oils, some of which have interesting, naturally-occurring functional groups, like castor oil,[18] or are conjugated, like tung oil.[19] Besides our main interest in vegetable oils, we have succeeded in incorporating agricultural by-products as reinforcing materials in bio-composites, making our materials greener.[20,21]

DISSERTATION ORGANIZATION

This thesis focuses on the study of several different vegetable oils, different polymerization techniques, and the use of cellulose nanowhiskers, all in the production of greener materials with the potential of replacing harmful petroleum-based polymers. The thesis is divided into six independent chapters. Chapter 1 is a general introduction that provides the major reasons for carrying out research in the area of bio-renewables and green chemistry. The following four chapters are the result of four different research projects in the area of vegetable oil-based materials. The final chapter summarizes our general conclusions derived from the different projects carried out during the past five years.

Chapter 2 addresses the synthesis and characterization of bio-plastics made with varying amounts of conjugated low saturation soybean oil (CLS), acrylonitrile (AN), and different dienes - dicyclopentadiene (DCP) and divinylbenzene (DVB) - via free radical polymerization using AIBN as an initiator. Chapter 3 describes the synthesis of 100% bio-based rubbery materials made with tung oil (TUN) and Ebecryl 860®, a commercially available acrylated soybean oil, and *tert*-butyl peracetate as the free radical initiator. Chapter 4 covers the development of a series of bio-rubbers polymerized by a cationic initiator (boron trifluoride diethyl ether, BFE). These rubbers contain high loads of conjugated soybean oil (CSO), styrene (ST), bio-diesel as a plasticizer, and various amounts of 1,5-hexadiene or isoprene as flexible crosslinkers. Chapter 5 reports the synthesis and characterization of castor oil-based waterborne polyurethanes reinforced with cellulose nanowhiskers, and a comparison of the physical and chemical properties introduced by incorporating the nanofiller chemically or physically.

The final chapter summarizes the major conclusions from Chapters 2-5. It also provides a wrap up for this thesis and enumerates some of the goals reached throughout my journey as a researcher at Iowa State University.

REFERENCES

[1] Bisio, A. L.; Xanthos, M. *How to Manage Plastics Wastes: Technology and Market Opportunities*. New York: Hanser Publishers, 1995.

[2] Mustafa, N. *Plastics Waste Management: Disposal, Recycling and Reuse*. New York: Marcel Dekker, 1993.

[3] Di Pierro, P.; Chico, B.; Villalonga, R.; Mariniello, L.; Damiao, A.; Masi, P.; Porta, P. Biomacromolecules 2006, 7, 744.

[4] Mohanty, A. K.; Liu, W.; Tummala, P.; Drzal, L. T.; Misra, M.; Narayan, R. "Soy Protein-based Plastics, Blends, and Composites." In: Mohanty, A. Misra, M., Drzal, L., editors. *Natural Fibers, Biopolymers, and Biocomposites*. Boca Raton: Taylor & Francis Group, 2005.

[5] Mizobuchi, Y. U.S. Patent 5395435; 1995.

[6] Bonacini, V. European Patent Office WO 02/44490 A1; 2002.

[7] Li, F.; Hanson, M. V.; Larock, R. C. Polymer 2001, 42, 1567.

[8] Formo, M. W. *Bailey's Industrial Oil and Fat Products*, Vol. 2. 4th Ed. New York: Wiley, 1982.

[9] Baber, T. M.; Vu, D. T.; Lira, C. T. J. Chem. Eng. Data 2002, 47, 1502.

[10] Li, F.; Larock, R. C. J. Appl. Polym. Sci. 2000, 78, 1044.

[11] Valverde, M.; Andjelkovic, D. D.; Kundu, P. P.; Larock, R. C. J. Appl. Polym. Sci. 2008, 107, 423.

[12] Williams, G. I.; Wool, R. P. Appl. Comp. Mat. 2000, 7, 421.

[13] Li, F.; Larock, R. C. Biomacromolecules 2003, 4, 1018.

[14] Andjelkovic, D. D.; Valverde, M.; Henna, P.; Li, F.; Larock, R. C. Polymer 2005, 46, 9674.

[15] (a) http://www.agmrc.org/commodities__products/grains__oilseeds/corn.cfm 6/2/2009 and
(b) http://www.agmrc.org/commodities__products/grains__oilseeds/soy/index.cfm 6/2/2009

[16] Lu, Y.; Larock, R. C. Biomacromolecules 2007, 8, 3108.

[17] Lu, Y.; Larock, R. C. Biomacromolecules 2008, 9, 3332.

[18] Valverde, M.; Lu, Y.; Larock, R. C. "Castor Oil-Based Waterborne Polyurethane Dispersions Reinforced with Cellulose Nanowhiskers," submitted to the *Journal of Applied Polymer Science.*

[19] Valverde, M.; Jackson, J. M.; Larock, R. C. "Free Radical Synthesis of Rubbers Made Entirely from Highly Unsaturated Vegetable Oils and Derivatives," submitted to the *Int. J. Polym. Mater.*

[20] Quirino, R. L.; Larock, R. C. J. Appl. Polym. Sci. 2009, 112, 2033.

[21] Pfister, D. P.; Baker, J. R.; Henna, P. H.; Lu, Y.; Larock, R. C. J. Appl. Polym. Sci. 2008, 108, 3618.

CHAPTER 2. CONJUGATED LOW SATURATION SOYBEAN OIL THERMOSETS: FREE RADICAL COPOLYMERIZATION WITH DCP AND DVB

A Paper Published in Journal of Applied Polymer Science, 107, 423-430.

Marlen Valverde, Dejan Andjelkovic, Patit P. Kundu, Richard C. Larock*

Department of Chemistry, Iowa State University, Ames, IA 50011, USA

Abstract

The free radical copolymerization of 40-85 wt % of conjugated low saturation soybean oil (CLS), and a 9:1 ratio of acrylonitrile (AN) and either divinylbenzene (DVB) or dicyclopentadiene (DCP) using AIBN as the initiator affords transparent yellow samples, which range from hard to slightly rubbery. DMA analysis indicates that the samples containing DCP have tan δ values ranging from 0.32 to 0.49, while the damping properties of the DVB samples are slightly lower. Extraction analysis shows that complete chemical incorporation of the CLS into the polymeric network is achieved when the original CLS content ranges from 40-65 wt %. Lower incorporation of the CLS into the polymer network occurs when the oil content exceeds 70 wt %. In this case, up to 30% of the CLS remains unreacted. These observations are supported by ^{1}H-NMR and solid state NMR. Thermogravimetric analysis (TGA) indicates a single stage degradation, implying that the polymer network is highly homogeneous in composition. The temperatures of 10% weight loss for the DCP system range from 402 to 428 ^{o}C, and from

370 to 391 ^{o}C for the DVB system. The temperature of maximum degradation ranges from 458 to 518 ^{o}C for the DCP polymers, and 406 to 422 ^{o}C for the DVB system.

1. Introduction

In recent years, there has been a growing demand for new starting materials for the fabrication of plastics and rubbers [1]. Until now, plastics have been primarily petroleum-based, which results in economic and environmental problems. Economic problems arise because petroleum is a finite resource and environmental issues result because the decomposition of these materials in nature is lengthy and sometimes generates by-products that are public hazards [1,2]. Recently, a growing number of bio-based substances have been shown under the proper reaction conditions to be viable alternatives to petroleum-based monomers. The most widely used are carbohydrates, like cellulose or chitin, and proteins, such as soy or cheese protein [3-5].

Materials made with these new bio-based monomers face a number of important challenges; particularly important is that their mechanical properties are better or at least comparable to those present in today's plastics and rubbers but more so, the potential capability of been biodegradable and/or biocompatible [5,6]. In the search for more and better options, the fatty acids present in vegetable oils are quite attractive, since they have been successfully introduced in the printing industry as part of fast drying inks [7], and as a glue for wood materials [8], but the synthesis of high molecular weight polymers has thus far been mostly unproductive [9].

Particularly promising as bio-based monomers are a wide variety of naturally occurring vegetable oils,[10] which consist of triglycerides differing primarily in their chain lengths and the number of carbon-carbon double bonds present in the triglyceride

unit [11]. The presence of the double bonds makes these oils suitable for polymerization, either by cationic [12] or free radical polymerization [13,14] processes. The reactivity of the oils towards different polymerization techniques depends on the number and nature of the double bonds. Conjugated double bonds are known to be more reactive towards these types of polymerizations [15].

The advantages of vegetable oils as polymeric starting materials include their low cost, ready availability, and annual renewability, as well as the possible biodegradability of the resulting polymeric materials after the targeted use [15]. The triglycerides have relatively high molecular weights before polymerization, plus a branched structure, so when polymerization does take place, viable crosslinked structures with considerable molecular weight are fairly easily attained.

Soybean oil is a biodegradable vegetable oil dominating today's food oil market. About 80% of the soybean oil produced each year is used for human food. Another 6% is used for animal feed, while the remainder (14%) serves nonfood uses (soaps, fatty acids, lubricants, coatings, etc.) [15]. The polyunsaturation of soybean oil and low saturation soybean oil (LSS) with still higher polyunsaturated fatty acid content [16] makes it possible to polymerize or copolymerize these natural oils into useful new materials [9,15,16].

The Larock research group has recently prepared and characterized a wide variety of plastic, elastomeric, adhesive, and rubbery materials by the copolymerization of regular soybean oil, low saturation soybean oil (LSS), and conjugated soybean oil [17,18]. These materials have been produced by cationic copolymerization of the oils with styrene (ST) and/or divinylbenzene (DVB) catalyzed by boron trifluoride diethyl

etherate (BFE) [9,17,19,]. These materials have room temperature moduli ranging from 6 $\times 10^6$ to 2 $\times 10^9$ Pa, and glass transition temperatures (T_g) ranging from 0 to 105 ^oC [18,20].

More recently, the thermal polymerization of highly reactive tung oil [21,22] and the free radical copolymerization of epoxidized acrylated soybean oil (Ebecryl ® 860) have been reported [23]. The free radical polymerization technique has always been appealing to industry, since it is a robust and generally cheap process that permits the use of a wide variety of monomers with or without relatively sensitive functionality due to the less rigorous reaction conditions it requires compared with other chain growth processes [24].

The C=C bonds of the LSS (averaging 5.1 per triglyceride unit [17]) are slightly more nucleophilic than those of ethylene and propylene and are susceptible to free radical polymerization. Upon conjugation of the C=C bonds by rhodium-catalyzed isomerization [25,26], conjugated LSS (CLS) is produced. These conjugated C=C bonds are even more reactive toward free radical polymerization. Thus, thermodynamically, the LSS and CLS oils, should be radically polymerizable monomers. The free radical polymerization of soybean oils should afford high molecular weight polymers with crosslinked polymer networks [27], since these oils themselves possess relatively high molecular weights with each of the unsaturated side chains of the triglyceride able to participate in free radical polymerization resulting in crosslinking. It should be noted that the allylic free radical intermediates produced by polymerization of the conjugated dienes in CLS are also considerably more stable that simple alkyl radicals [28].

Recently our research group has also been successful in synthesizing polymers by the free radical copolymerization of conjugated linseed oil (CLIN), AN, and DVB [13]. Although the chemical approach involved in this project is very similar, the properties of the materials are quite different. In this paper, we wish to report our recent results on the free radical copolymerization of CLS, AN, and either dicyclopentadiene (DCP) or DVB. A variety of light yellow, transparent polymeric materials ranging from elastomers to tough and rigid plastics have been prepared by varying the stoichiometry. The synthesis, structure, and thermophysical properties of these new materials are reported herein.

2. Experimental Section

2.1. Materials

The LSS (Select Oil®) oil used in this study is a food-grade oil supplied by Zeeland Food Service, Inc. (Zeeland, MI), and purchased in the local supermarket. The CLS has been prepared by rhodium-catalyzed isomerization of the LSS oil [25,25]. The percent conjugation is calculated to be ~ 100%. The DVB comonomer was purchased from Aldrich Chemical Company as a mixture of 80% DVB and 20% ethylvinylbenzene, and used as received. The AN and DCP comonomers were purchased from Aldrich Chemical Company, and used as received.

2.2. Methods

2.2.1. Polymer Preparation and Nomenclature.

Varying amounts of CLS, AN, and DCP or DVB were mixed in a cylindrical glass vial with 1 wt % 2,2′-azobis(isobutyronitrile) (AIBN). The amount of CLS oil has been varied from 40 to 85 wt %. The ratio of the AN to DVB or DCP was held at 9 to 1. The vial was heated first at 60 °C for 12 h, then at 70 °C for 12 h, 80 °C for 12 h, 90 °C for 12 h, and finally 110 °C for 12 h. This prolonged heating sequence was necessary to avoid substantial cracking and shrinking. The nomenclature adopted in this work for the polymer samples is as follows; a polymer sample prepared from 50 wt % CLS, 45 wt % AN, 5 wt % DVB, and 1 wt % AIBN is designated as CLS50-AN45-DVB5-AIBN1.

2.2.2. Soxhlet Extraction. A 2 g sample of the bulk polymer was extracted for 24 h with 100 mL of refluxing methylene chloride using a Soxhlet extractor. After extraction, the resulting solution was concentrated by rotary evaporation and subsequent vacuum drying. The soluble substances were characterized further by ^{1}H NMR spectroscopy. The insoluble materials remaining after extraction were dried under vacuum for several hours before weighing and subsequent characterization by ^{13}C NMR spectroscopy.

2.2.3. Gel Permeation Chromatography. All molecular weights (relative to narrow polystyrene standards) were measured using a Waters Breeze GPC system equipped with a Waters 1515 pump, Waters 717-plus autosampler, and Waters 2414 RI detector. HPLC grade THF was used as the mobile phase at a flow rate of 1 mL/min with a sample injection volume of 200 μL. HPLC analyses were carried out using a set of two columns (PL-Gel Mixed C 5 μm, Polymer Lab., Inc.) heated at 40 °C. Prior to analysis, each

polymer sample was dissolved in THF (~2.0 mg/mL) and passed through a Teflon 0.2 mm filter into a sample vial.

2.2.4. ^{1}H NMR Spectroscopic Characterization. The ^{1}H NMR spectra of the extracted soluble substances were obtained in $CDCl_3$ using a Varian Unity spectrometer at 300 MHz.

2.2.5. GC Analysis. An HP6890 series gas chromatograph (Hewlett Packard Co., Wilmington, DE) equipped with an autosampler and flame ionization detector was used for analysis of the LSS and CLS oils. A SUPELCOWAX^{TM}-10 capillary column (30 m × 0.25 mm × 0.25 μm film thickness, Supelco, Bellefonte, PA) was used for separation.

2.2.6. Dynamic Mechanical Analysis (DMA). All DMA data were obtained using a Perkin-Elmer dynamic mechanical analyzer DMA Pyris-7e in a three-point bending mode. Rectangular specimens were made by copolymerizing the reactants in a cylindrical mold and then cutting and sanding them down to the appropriate sample shape. Thin sheet specimens of 1 mm thickness and 5 mm depth were used, and the width to depth ratio was maintained at approximately 2. The measurements were performed at a heating rate of 3 °C/min from -40 ^{o}C to 250 ^{o}C and a frequency of 1 Hz in helium (20 mL/min). The crosslink densities were determined from the rubbery modulus plateau based on the theory of rubber elasticity [29].

2.2.7. Thermogravimetric Analysis (TGA). A Perkin-Elmer Pyris-7 thermogravimeter was used to measure the weight loss of the polymeric materials in air (20 mL/min). The samples were heated from 50 to 650 °C at a heating rate of 20 °C/ min.

3. Results and Discussion

The LSS oil is a triglyceride oil composed of esters comprising approximately 19% oleic acid (one C=C), 63% linoleic acid (two C=C), 9% linolenic acid (3 C=C) with ~ 5.1 C=C per triglyceride unit [17]. By conjugating the carbon-carbon double bonds in the triglyceride side chains of the natural oil, their reactivity can be significantly improved. The LSS oil has been conjugated using a published procedure [25,25] to produce the CLS oil.

GC analyses of the LSS and CLS oils indicate that the conjugation process affords primarily two conjugated linoleic acid (CLA) isomers. *Cis*-9,*trans*-11 CLA and *trans*-10,*cis*-12 CLA are the predominant isomers present after conjugation (Table I), indicating that during conjugation only one double bond moves and it ends up *trans*. The amounts of the different CLA isomers indicate that the two different double bonds of the linoleic acid have an equal tendency to move towards the other double bond, since both isomers are present in ~27% in the CLS oil. These findings are in agreement with work recently reported by us on the conjugation of several different vegetable oils [25].

Table I

GC Analysis of the Fatty Acid Content of LSS Before and After Conjugation (CLS) [2,4].

Fatty acid	LSS (%)	CLS (%)
Linoleic acid (C18:2)	63.2	0.5
cis-9,*trans*-11 CLA	--	26.1
trans-10,*cis*-12 CLA	--	28.0

Rigid, hard, and transparent yellow plastics have been produced by the free radical copolymerization of the CLS oil with AN, and either DVB or DCP. The latter three olefins are all monomers suitable for free radical polymerization. The DVB molecule has two carbon-carbon double bonds that are in conjugation with a benzene ring, making this comonomer quite reactive towards free radical polymerization. On the other hand, DCP possesses two double bonds in a bicyclic skeleton, which are not in conjugation, but their reactivity towards free radical polymerization is still considerable due to the strain present in the bicyclic system. The copolymerization of mixtures of AN and DVB or DCP with the CLS oil results in hard plastic materials when as little as 1.5-6 wt % DVB or DCP are employed.

The preparation of the samples is very simple. All of the reagents are mixed in a glass vial along with the free radical initiator. Polymerization is initiated when the samples are placed in an oil bath at 60 ^{o}C, a temperature appropriate for AIBN decomposition to free radicals. To avoid any formation of bubbles or cracks and to avoid

major shrinkage of the samples during the heating sequence, a lengthy cure time is required and only very gradual increases in the cure temperature have been employed. The samples have been cured by heating them successively in 12 hour periods at 60, 70, 80, 90, and 110 ^{o}C. Sheme 1 illustrates the random polymer network formed upon the copolymerization of CLS, AN, and DCP.

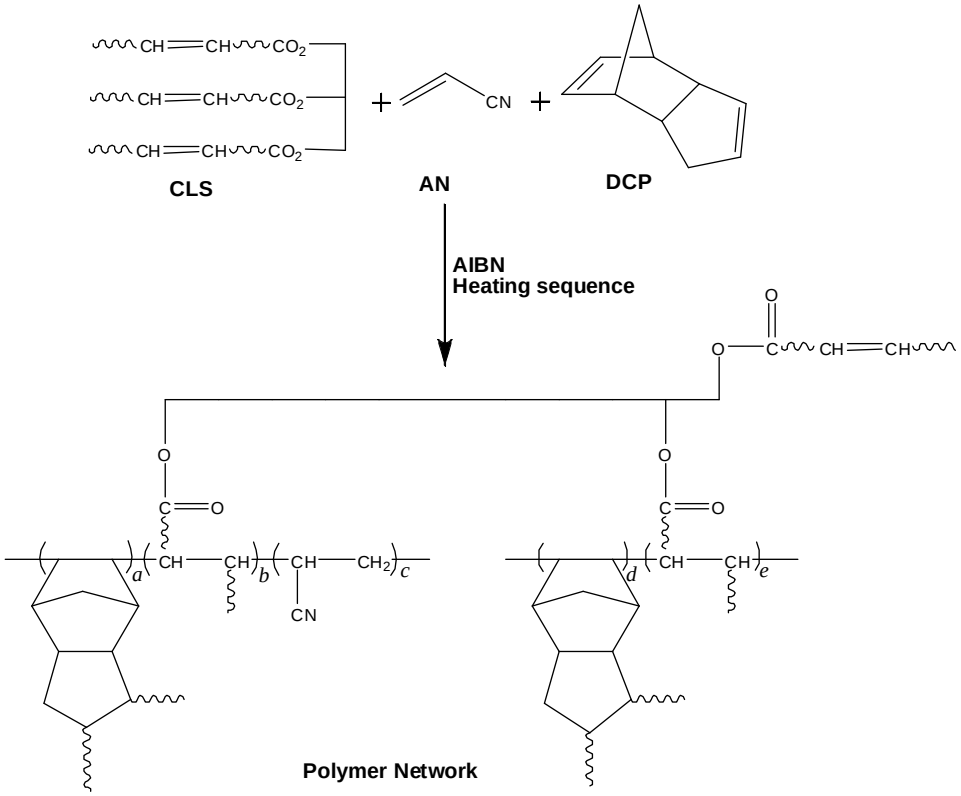

Scheme 1. Polymerization of CLS, AN, and DCP.

Soxhlet extraction of the samples has been performed to determine the amount of CLS and other comonomers that are not incorporated into the polymer network as crosslinked materials. The results of the Soxhlet extraction for both the DVB and DCP systems are shown in Tables II and III respectively. As the amount of CLS increases from

40 to 85 wt %, the amount of soluble material increases as well, increasing from 5 to 34% in the case of the DVB samples, and from 1 to 33% for the DCP samples. This increase in soluble materials when adding more CLS oil suggests that this soluble material is mainly unreacted CLS oil. Indeed, ^{1}H NMR spectroscopic analysis of the soluble materials indicate that only CLS oil is present; we were unable to find any peaks belonging to AN, DVB, or DCP, either because they simply are not present or because their concentration is so low that the peaks due to the CLS oil overlap them completely.

Table II

Extraction and Dynamic Mechanical Analysis Data for Samples Prepared from DVB.

Sample	T_g (^{o}C)	Tan delta	Temp. range[a] (^{o}C)	ν_e (10^3mol/m^3)	Sol %	Insol %
CLS40-AN54-DVB6-AIBN1	104	0.35	80-130	109	4.9	96.6
CLS50-AN45-DVB5-AIBN1	101	0.32	75-115	73	4.9	95.1
CLS55-AN40-DVB4.5-AIBN1	85	0.33	65-100	72	5.1	95.1
CLS60-AN36-DVB4-AIBN1	74	0.38	70-90	74	5.9	94.0
CLS65-AN31.5-DVB3.5-AIBN1	56	0.36	40-77	68	7.4	93.1
CLS70-AN27-DVB3-AIBN1	48	0.38	15-50	57	9.9	91.0
CLS75-AN22.5-DVB2.5-AIBN1	25	0.38	0-35	43	15.5	85.5
CLS80-AN18-DVB2-AIBN1	2	0.41	-35-27	31	20.1	80.8
CLS85-AN13.5-DVB1.5-AIBN1	-30	0.49	-40-0	20	33.8	66.8

[a] Temperature range in which the tan delta values are above 0.3.

Table III

Extraction and Dynamic Mechanical Analysis Data for Samples Prepared from DCP.

Sample	T_g (^oC)	Tan delta	Temp. range[a] (^oC)	ν_e ($10^3 mol/m^3$)	Sol %	Insol %
CLS40-AN54-DCP6-AIBN1	107	0.49	82-140	59	0.9	99.1
CLS50-AN45-DCP5-AIBN1	84	0.45	75-125	60	1.8	98.2
CLS55-AN40-DCP4.5-AIBN1	67	0.44	60-110	31	2.9	97.1
CLS60-AN36-DCP4-AIBN1	65	0.46	50-90	31	2.7	97.3
CLS65-AN31.5-DCP3.5-AIBN1	48	0.48	17-71	23	4.6	95.4
CLS70-AN27-DCP3-AIBN1	32	0.47	0-50	19	7.5	92.5
CLS75-AN22.5-DCP2.5-AIBN1	20	0.53	-8-40	20	12.4	87.6
CLS80-AN18-DCP2.0-AIBN1	-7	0.51	-40-10	20	19.9	80.1
CLS85-AN13.5-DCP1.5-AIBN1	-32	0.52	-40--5	18	32.5	71.3

[a] Temperature range in which the tan delta values are above 0.3.

Soxhlet extraction separated the insoluble materials from the soluble, unreacted CLS oil. These insoluble materials are the crosslinked polymer networks, which must be composed of CLS oil, AN, and DVB or DCP. The insoluble portions have been analyzed by solid state ^{13}C NMR spectroscopy. As shown in Figure 1 for the sample CLS70-AN27-DCP3-AIBN1, there is evidence at 30-50 ppm for C-H bonds. The peak between 100 and 150 ppm corresponds to C=C carbons apparently left unreacted in the starting materials. The peaks between 150 to 175 ppm correspond to nitrile groups arising from

the AN, and the peaks above 200 ppm correspond to the ester moieties present in the backbone of the triglyceride unit.

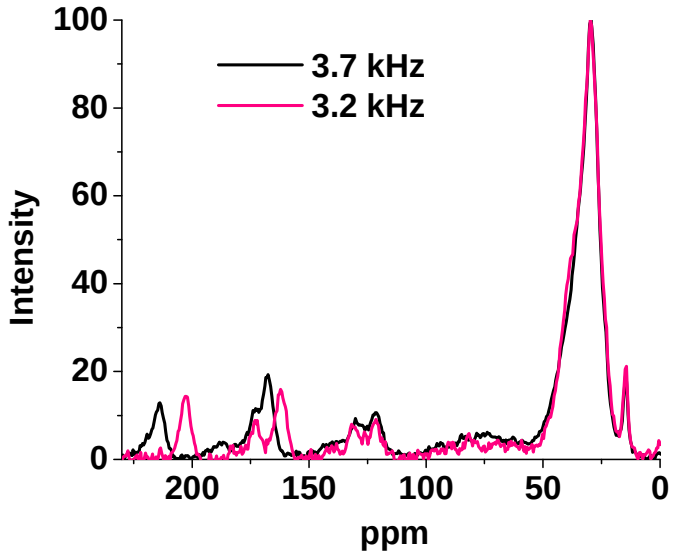

Figure 1. ^{13}C NMR spectra of the insoluble materials from CLS70-AN27-DCP3-AIBN1.

GPC analyses performed on some of the soluble samples show that the soluble portions removed during Soxhlet extraction constitute mainly three different kinds of molecules. Figure 2 presents the GPC chromatogram of four samples and the original CLS oil. Three major peaks are present. Peak A corresponds to molecules that have a relatively low molecular weight. Since this analysis was performed utilizing polystyrene standards, the molecular weight values calculated by the instrument are only an approximation. These low molecular weight molecules are not present in the pure CLS oil, which indicates that these smaller molecules appear as a consequence of the free radical polymerization process itself. It is possible that the triglycerides present in the oil undergo some kind of degradation that liberates fatty acids or fractions of the fatty ester

chains or these peaks may be due to oligomerization of the various starting monomers. The peak labeled as B corresponds to the largest portion of molecules present in the extracts and it is also present in the CLS oil, suggesting that this peak corresponds to the triglycerides that make up this vegetable oil, further establishing that the soluble portions of the samples in this study are composed mainly of unreacted vegetable oil. Finally, a third peak appears (peak C), having essentially twice the molecular weight of peak B, suggesting that this peak is due to triglyceride dimers, which are also present in the pure CLS oil. This dimer is apparently not a result of the polymerization process itself.

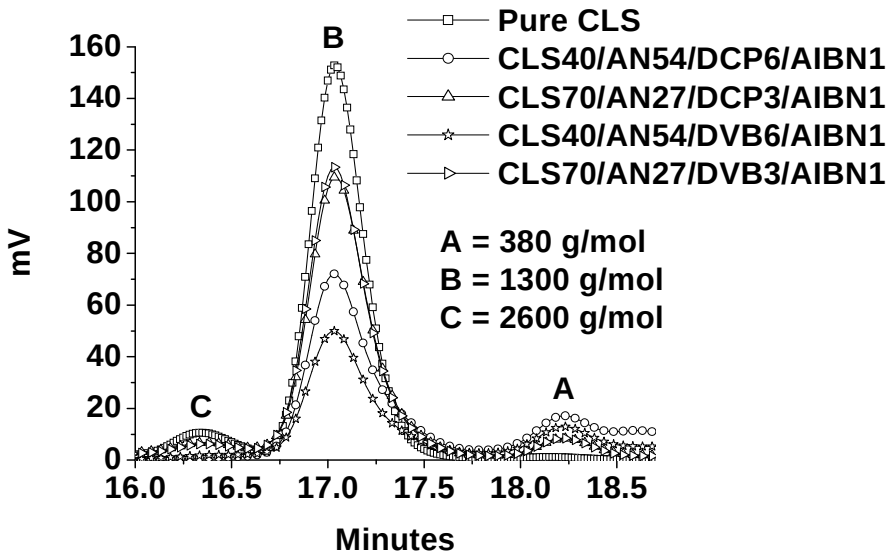

Figure 2. GPC analysis of the soluble extracts.

The glass transition temperatures of the samples prepared using DVB (Table II) and DCP (Table III) decrease steadily as the amount of CLS oil increases. As explained earlier, the amount of unreacted oil within the polymer network increases as the amount of CLS oil in the original composition increases. This unreacted oil can act as a

plasticizer for the materials. Therefore, the samples with a higher concentration of the CLS oil show lower T_g's. The plasticizer allows more segmental movement of the incorporated comonomers. This increment in segmental movement shows up as a decrease in the T_g value, which for the DVB samples range from 104 to -30 ^oC, and for the DCP samples range from 107 to -32 ^oC. This means that the DVB or DCP does not have much influence on the T_g's, since the values for both systems are fairly similar when comparing samples with identical compositions.

The viscoelastic properties of these thermosets make them suitable for use as damping materials [29], because of their ability to dissipate mechanical energy. The tan delta (δ) values for the DVB and DCP systems are reported in Tables 2 and 3 respectively. The higher tan δ values are obtained for the DCP-derived materials; they range from 0.43 to 0.53. The DVB system affords tan delta values between 0.32 and 0.49. Thus, the DCP materials have a higher capability for absorbing vibrations and dissipating energy inside the polymer network. It is generally accepted that materials with tan delta values above 0.3 are considered good damping materials [29]. Both the DCP and DVB systems exceed this limit, but the DCP system affords slightly higher values using identical compositions. Thus, DCP has several advantages, since it is much less expensive, and also affords better damping properties. It is also worth noting that the highest values of tan delta for both systems were obtained for the samples with higher amounts of the CLS oil (85 wt %), which is also an advantage from a biorenewable point of view. This finding is very important, because these plastics with a high content of the inexpensive vegetable oil show characteristics comparable to those of petroleum-based plastics.

In Tables II and III, the temperature range at which the samples have a tan δ value above 0.3 are reported. As the content of the CLS oil increases, the temperature range for good damping decreases, presumably because the CLS oil acts as a plasticizer, which lowers the T_g (taken at the highest point of the tan δ curve) of the material, making it softer as the temperature range falls below room temperature.

Another parameter that varies with the content of the CLS oil is the crosslink density. The DVB system (Table II) has crosslink densities that vary from 109×10^3 to 20 $\times 10^3$ mol/m^3. The higher values correspond to the samples with less CLS oil or with more AN and DVB, which are better crosslinkers compared to the CLS oil. Since the triglyceride CLS oil has approximately 5.1 total carbon-carbon double bonds and possesses a considerably higher molecular weight than either the AN (1 double bond) or DVB (2 double bonds that can act as crosslinking units), it has a lower crosslinking ability per molecular weight unit compared to the two other comonomers. The crosslink densities of the samples prepared from DCP range between 18 x 10^3 to 60 x 10^3 mol/m^3. The values decrease as the amount of CLS oil increases for both systems, since the amount of AN and DCP or DVB has to be lowered in order to keep the 9 to 1 AN-crosslinker ratio constant. It is also observed that the DCP samples have crosslink densities lower than those of the DVB samples; thus, DCP is not as good a crosslinker as DVB.

All of the samples described here are relatively thermally stable below 200 ^{o}C. They all undergo a three stage degradation process (Figure 3). The first stage from 30 to approximately 350 ^{o}C represents the loss of loosely bound molecules, such as the

unreacted CLS oil or small oligomers. The second stage involves degradation of the bulk polymer network, and the third stage involves degradation of the char residue. Thermogravimetric analysis (TGA) data indicates that these thermosets lose approximately 10% of their original mass below 400 ^{o}C for the DCP system (Table 4), and at a slightly lower temperature for the DVB system (Table 5). The 10% weight loss of these samples corresponds to the loss of volatile, relatively low molecular weight materials, mostly unreacted CLS oil or lower molecular weight oligomers.

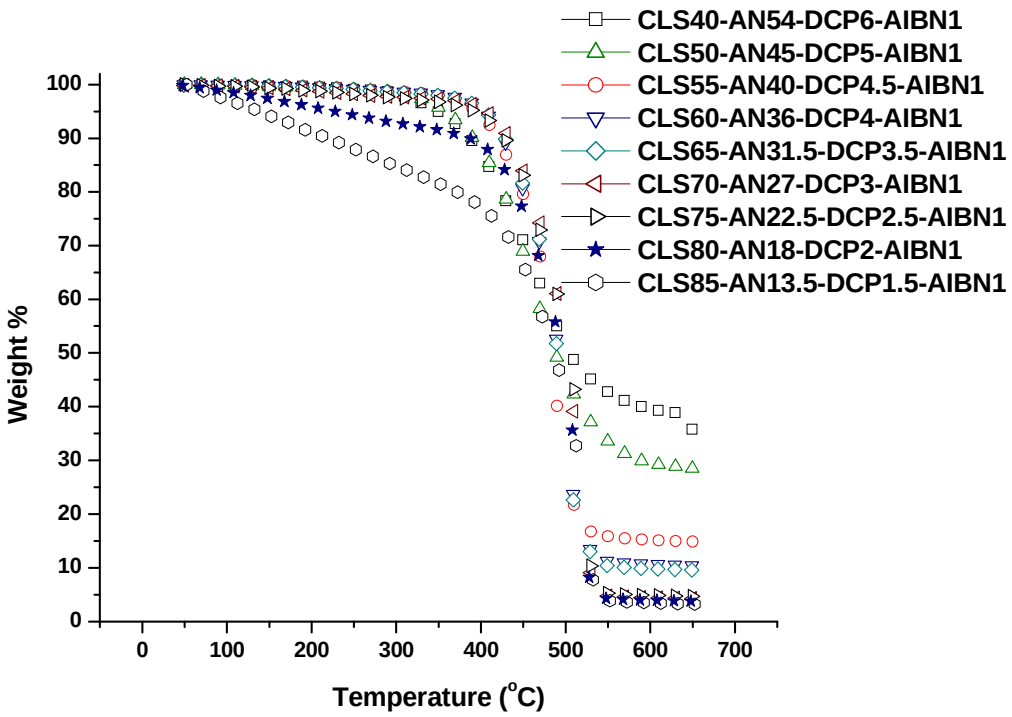

Figure 3. TGA curves for the DCP samples.

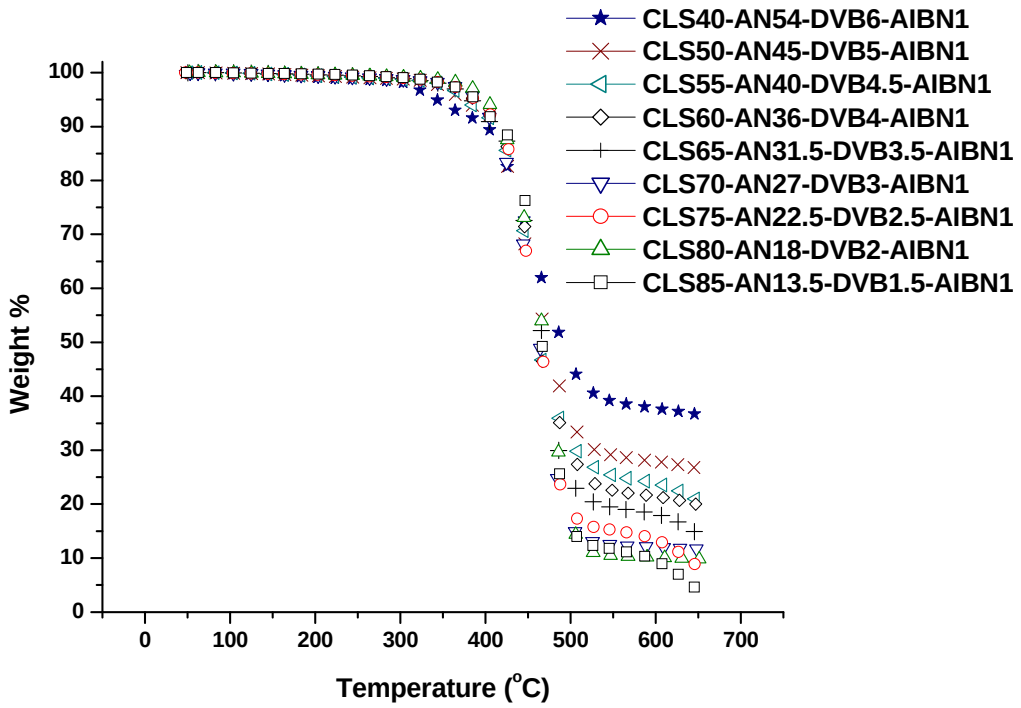

Figure 4. TGA curves for the DVB samples.

For the DCP system, the values of 50% weight loss, which as stated earlier correspond to degradation of the bulk polymer network of the materials, are somewhat higher than those of the DVB system. One reason for this difference could be the amount of energy that needs to be applied to the polymer network to degrade it. The degradation process is understood as the breakage or failure of bonds between atoms that hold together a material and, as consequence of this, small molecules escape the matrix giving rise to the lost of mass.

The temperature of maximum degradation follows the same trend as the temperature of 50% degradation; the DCP-containing systems exhibit higher temperatures, which are opposite to what one would expect, since the crosslink densities are lower than those of the corresponding DVB samples.

It is also important to point out that the quantity of material (char) left after the heating process diminishes as the amount of CLS oil increases in the original composition. This phenomenon can be observed in both the DVB and the DCP systems; see Figures 4 and 5. The most logical reason for this is that the char residue is composed mainly of AN, DVB, and/or DCP, which are the components that decrease as the CLS oil content is increased.

Table IV

Thermogravimetric Analysis of the DCP Samples.

Sample	Temp. of 10% degradation (^{o}C)	Temp. of 50% degradation (^{o}C)	Temp. Interval (^{o}C)	Temp. of max. degradation rate (^{o}C)
CLS40-AN54-DCP6-AIBN1	402	490	88	460
CLS50-AN45-DCP5-AIBN1	419	484	65	490
CLS55-AN40-DCP4.5-AIBN1	421	490	69	496
CLS60-AN36-DCP4-AIBN1	426	491	65	499
CLS65-AN31.5-DCP3.5-AIBN1	428	490	62	499
CLS70-AN27-DCP3-AIBN1	411	463	52	458
CLS75-AN22.5-DCP2.5-AIBN1	413	464	51	461
CLS80-AN18-DCP2-AIBN1	427	502	75	518
CLS85-AN13.5-DCP1.5-AIBN1	210	488	278	462

Table V

Thermogravimetric Analysis of the DVB Samples.

Sample	Temp. of 10% degradation (^{o}C)	Temp. of 50% degradation (^{o}C)	Temp. Interval (^{o}C)	Temp. of maximum degradation rate (^{o}C)
CLS40-AN54-DVB6-AIBN1	376	463	87	406
CLS50-AN45-DVB5-AIBN1	370	471	101	458
CLS55-AN40.5-DVB4.5/AIBN1	373	462	89	453
CLS60-AN36-DVB4-AIBN1	380	462	82	456
CLS65-AN31.5-DVB3.5/AIBN1	378	470	92	465
CLS70-AN27-DVB3.0-AIBN1	382	450	68	424
CLS75-AN22.5-DVB2.5-AIBN1	390	469	79	432
CLS80-AN18-DCV2-AIBN1	391	464	73	454
CLS85-AN13.5-DVB1.5-AIBN1	407	466	59	457

In general, the samples prepared using DCP appear to be more rubbery than the DVB samples. This physical observation correlates well with the values found for the crosslink densities. It appears that DVB is a better crosslinker. As the amount of CLS oil increases in the composition of the sample, the softer the material appears. This characteristic is mainly due to two features. First, the higher CLS oil content results is less of the AN, and the more reactive crosslinker DVB or DCP. Therefore, there is less chance to form crosslinks. Secondly, as the amount of CLS oil increases, the amount of

unreacted oil increases as well. This unreacted oil acts as a plasticizer, lowering the T_g from above 100 ^oC to around -30 ^oC for both systems. These two features result in the DCP samples having higher tan δ values, suggesting that these new vibration-absorbing, bio-based polymeric materials have potential industrial applications as damping materials. For example, they might be used in automobile parts, like door panels, to isolate the interior from the vibration-producing exterior. Due to the softness of the DCP samples, it is easier to process them and produce samples in a desired shape.

The samples prepared from DVB are more rigid than the ones prepared from DCP. Other than this difference, both systems have similar transparency, coloration, and odor. None of the samples are oily; all samples are glossy and smooth to the touch.

Since the free radical initiator AIBN releases nitrogen gas upon decomposition, some samples contain voids or bubbles trapped within the samples. To prevent formation of these bubbles, the volume of the glass mold (vial) in which the samples were prepared had to be increased, so the N_2 released had more space to escape from the curing resin. Another problem found during the synthesis of these materials was the development of cracks, particularly when the samples were prepared in plate-like glass molds. The formation of cracks is presumably due to the presence of AN. When AN polymerizes, it shrinks, causing contraction of the resin inside a confined space, which gives rise to cracks. This problem was not observed in cylindrical samples, so all the work reported here was performed on this shape sample.

One of the major advantages of using DCP is that it is a substantially cheaper starting material – $0.29 per pound compared to $3.00 per pound for DVB [30]. One disadvantage of employing DCP is the lower crosslink density which results. On the other

hand, it appears that the reactivity of both the CLS and DCP are very similar. Overall there is better chemical incorporation of the CLS oil when using DCP compared to DVB.

4. Conclusions

Promising new bio-based plastics have been prepared from CLS, AN and either DCP or DVB. Chemical incorporation of the CLS oil into the polymeric network reaches almost 100% when the oil content is between 40-65 wt %, especially for the DCP samples. Lower percentages of oil incorporation into the network are achieved when the oil content is 85 wt %. In this case, 20-30% of the original oil remains soluble. DCP gives higher tan delta values than the DVB thermosets when comparing the same sample composition. The DCP samples have higher chemical incorporation of the CLS oil in the polymer network, which improves vibrational damping, since the longer triglyceride molecules dissipate vibrations better. The comparable T_g values found for the DCP and DVB systems suggest that DVB and DCP comonomers do not have much influence on the behavior of the T_g's when comparing the same sample compositions.

Acknowledgments

The authors wish to thank Dr. Surya Mallapragada from the Department of Materials Science and Engineering at Iowa State University, Drs. Jay-Lin Jane and Perminas Mungara from the Department of Food Science and Human Nutrition at Iowa State University, and the funding agencies, which supported this research, the United States Department of Agriculture, Archer Daniels Midland, and the Illinois-Missouri Biotechnology Alliance.

References

[1] Bisio, A. L.; Xanthos, M. How to Manage Plastics Wastes: Technology and Market Opportunities. New York: Hanser Publishers, 1995.

[2] Mustafa, N. Plastics Waste Management: Disposal, Recycling and Reuse. New York: Marcel Dekker, 1993.

[3] Di Pierro, P.; Chico, B.; Villalonga, R.; Mariniello, L.; Damiao, A.; Masi, P.; Porta, P. Biomacromolecules 2006; 7: 744-749.

[4] Mohanty, A. K.; Liu, W.; Tummala, P.; Drzal, L. T.; Misra, M.; Narayan, R. Soy Protein-based Plastics, Blends, and Composites. In: Mohanty A.; Misra M.; Drzal L. editors. Natural Fibers, Biopolymers, and Biocomposites. Boca Raton. Taylor & Francis Group, 2005. pp. 699.

[5] Neto, C. G. T.; Giacometti, J. A.; Job, A. E.; Ferreira, F. C.; Fonseca, J. L. C.; Pereira, M. R. Carbohyd. Polym. 2005; 62: 97-103.

[6] Zhang, K.; Wang, Y. ; Hillmyer, M. A. ; Francis, L. F. Biomaterials 2004; 25: 2489–2500.

[7] Mizobuchi, Y. US Patent 5395435; 1995.

[8] Bonacini, V. European Patent Office WO 02/44490 A1; 2002.

[9] Li, F. ; Hanson, M. V.; Larock, R. C. Polymer 2001; 42: 1567-1579.

[10] Can, E.; Wool, R. P.; Kusefoglu, S. J. Appl. Polym. Sci. 2006, 102, 2433.

[11] Formo, M. W. in: Swern, D, editor. Bailey's Industrial Oil and Fat Products, vol. 2. 4th ed. New York: Wiley, 1982, pp 343–405.

[12] Li, F.; Larock, R. C. J. Appl. Polym. Sci. 2000; 78: 1044-1056.

[13] Henna, P. H.; Andjelkovic, D. D.; Kundu, P. P.; Larock, R. C. J. Appl. Polym. Sci. 2007, 104, 979-985.

[14] Williams, G. I.; Wool, R. P. Appl. Comp. Mat. 2000; 7: 421-432.

[15] Li, F. Larock, R. C. 'Synthesis, Properties, and Potential Applications of Novel Thermosetting Biopolymers from Soybean and Other Natural Oils." In: Mohanty A, Misra M.; Drzal L. editors. Natural Fibers, Biopolymers, and Biocomposites. Boca Raton. Taylor & Francis Group, 2005, pp. 727.

[16] Reske, J.; Siebrecht, J.; Hazebroek, J. J. Am. Oil Chem. Soc. 1997; 74: 989-998.

[17] Li, F.; Larock, R. C. J. Polym. Sci. B. Polym. Phys. 2001; 39: 60-77.

[18] Andjelkovic, D. D.; Valverde, M.; Henna, P.; Li, F.; Larock, R. C. Polymer 2005; 46: 9674-9685.

[19] Li, F.; Hanson, M.V. ; Larock, R. C. Polymer 2001; 42: 1567-1579.

[20] Li, F.; Larock, R. C. J. Appl. Polym. Sci. 2001; 80: 658-670.

[21] Li, F.; Larock, R. C. Biomacromolecules 2003; 4: 1018-1025.

[22] Kundu, P. P.; Larock, R. C. Biomacromolecules 2005; 6: 797-806.

[23] Khot, S. N.; Lascala, J. J.; Can, E.; Morye, S. S.; Williams, G. I.; Palmese, G. R.; Kusefoglu, S. H.; Wool, R. P. J. Appl. Polym. Sci. 2001 ; 82: 703-723.

[24] Billmeyer, F. W. Textbook of Polymer Science, 2nd ed. New York: Wiley-Interscience, 1971, pp 282-283.

[25] Andjelkovic, D. D.; Min, B.; Ahn, D.; Larock, R. C. J. Agric. Food. Chem. 2006; 54, 9535.

[26] Larock, R.C.; Dong, X.; Chung, S.; Reddy, C. R.; Ehlers, L. E. J. Am. Oil Chem. Soc. 2001; 78: 447-453.

[27] Li, F.; Marks, D. W.; Larock, R. C.; Otaigbe, J. U. Polymer 2000; 41: 7925-39.

[28] Painter, M. “Fundamentals of Polymer Science.” Wiley: New York, 1998.

[29] Nielsen, L. E.; Landel, R. F. “Mechanical Properties of Polymers and Composites,” 2nd ed.; Marcel Dekker: New York, 1994.

[30] Chemical Market Reporter, ICIS Publications: New York, March 21, 2005.

CHAPTER 3. FREE RADICAL SYNTHESIS OF RUBBERS MADE ENTIRELY FROM HIGHLY UNSATURATED VEGETABLE OILS AND DERIVATIVES

A Paper to be Published in the International Journal of Polymeric Materials

Marlen Valverde, Joy M. Jackson, and Richard C. Larock*

Department of Chemistry, Iowa State University, Ames. IA 50011

Abstract

The free radical copolymerization of 100% bio-based samples containing 10 to 90 wt % tung oil and 90 to 10 wt % of Ebecryl 860 using t-butyl peracetate as the initiator affords transparent yellow samples, which range from hard to soft rubbers. DMA analysis indicates that the samples exhibit higher tan delta values as the amount of tung oil increases in the initial composition; the values range from 0.3 to ~1.0. Extraction analysis indicates that as the amount of tung oil increases in the initial composition, increasing amounts of this oil are obtained upon extraction. The tung oil evidently acts as a plasticizer, since these rubbery materials become softer as the wt % of tung oil increases. Thermogravimetric analysis shows only a single stage thermal degradation, indicating that these materials are highly homogeneous in composition. These materials are quite thermally stable below 350 ^{o}C and exhibit temperatures of 10% weight loss ranging from 375 to 425 ^{o}C. The temperature of 50% weight loss ranges from 445 to 485 ^{o}C. Compression analyses show that the stress values range from 2 to 86 MPa, and the strain values from 25 to 46%.

INTRODUCTION

In recent years, the scientific community has increasingly focused its efforts on the development of biorenewable materials for the fabrication of plastics and rubbers [1]. Until now, plastics have been primarily petroleum-based, which results in the economic and environmental problems we are all familiar with. Recently, a growing number of bio-based substances have been shown, under the proper reaction conditions, to be viable alternatives to petroleum-based monomers for the production of useful plastics. Carbohydrates, like cellulose or chitin [2], and proteins, such as soy [3] or cheese protein [4], are examples.

In the search for newer options, the fatty acids present in vegetable oils are quite attractive, since they have been successfully introduced in the printing industry as part of fast drying inks [4], and as a glue for wood materials [5], but the synthesis of high molecular weight polymers from these materials has only recently been achieved [6].

Vegetable oils appear to be particularly promising as bio-based monomers. They consist of triglycerides differing primarily in their chain lengths and the number of carbon-carbon double bonds present in the triglyceride unit [7]. The presence of the double bonds makes these oils suitable for polymerization, either by cationic [8] or free radical [9,10] polymerization processes, and, if enough double bonds are present and they are conjugated, even simple thermal polymerization is possible [11]. The reactivity of the oils towards different polymerization techniques depends on the number and nature of the double bonds. Conjugated double bonds are known to be more reactive towards these types of polymerizations [12].

Our research group has recently prepared and characterized a wide variety of plastic, elastomeric, adhesive, and rubbery materials made from a variety of vegetable oils. We have also succeeded in producing thermosets by the thermal copolymerization of highly reactive tung oil [11,13]. The free radical copolymerization of epoxidized acrylated soybean oil (commercially available as Ebecryl 860) has been reported by Wool and co-workers [14]. Free radical polymerizations are particularly appealing to industry, since they are robust and generally cheap processes that permit the use of a wide variety of monomers with or without relatively sensitive functionality due to the less rigorous reaction conditions required when compared with other chain growth processes [15].

Tung oil is readily available as a major product from the seeds of the tung tree. This oil is a triglyceride composed mainly (~84%) of alpha-elaeostearic acid (*cis*-9, *trans*-11, *trans*-13-octadecatrienoic acid). The high unsaturation and conjugation of the C=C bonds in tung oil makes this an excellent drying oil at room temperature [8,11].

Ebecryl 860 is a chemically modified soybean oil, which possesses -OH groups and acrylate functionality where the natural double bonds of the triglyceride used to be. The acrylate functionality enhances the reactivity of the triglyceride towards free radical polymerization. The synthesis of this modified vegetable oil has previously been reported by Wool *et. al.* [14].

The present work describes the conversion of tung oil and Ebecryl 860 into sturdy rubbers by free radical copolymerization using *t*-butyl peracetate (TBPA) as the initiator. We also present chemical and mechanical data that further describe the properties associated with these interesting new bio-renewable materials.

EXPERIMENTAL

Materials

The tung oil used in this study was obtained from Archer Daniels Midland (ADM) and used as received without any further purification. The acrylated epoxidized soybean oil (Ebecryl 860) was supplied by UCB Chemicals. The free radical initiator *t*-butyl peracetate (TBPA) was purchased from Aldrich Chemical Company, and used as received. All of the oils utilized and their mixtures were kept in dark containers under refrigeration to prevent any possible self polymerization.

Preparation of Samples

The mixtures of the oils and the initiator were placed in cylindrical glass molds, and heated in a programmable oven. The temperature was held at 80 ^{o}C for 12 h, then increased from 80 to 200 ^{o}C and heated at that temperature for 4 h, and finally the samples were kept at 200 ^{o}C for 12 more hours.

Characterization

Dynamic mechanical analysis data were obtained using a Perkin-Elmer dynamic mechanical analyzer, DMA Pyris-7e, in a three-point bending mode. Rectangular specimens were carried out by copolymerizing the reactants in an appropriate mold. Thin sheet specimens of 1 mm thickness and 2.5 mm depth were used, and the width to depth ratio was maintained at approximately 5. All ^{1}H NMR spectra were recorded in $CDCl_3$ using a Varian Unity spectrometer at 300 MHz. Extractions were made using a 2 g

sample of the bulk polymer and 100 mL of refluxing methylene chloride for 24 h in a Soxhlet extractor. After extraction, the resulting solution was concentrated by rotary evaporation and subsequent vacuum drying. The soluble substances were characterized further by ^{1}H NMR spectroscopy. The insoluble materials remaining after extraction were dried under vacuum for several hours before weighing. A Perkin-Elmer Pyris-7 thermogravimeter was used to measure the weight loss of the polymeric materials in air (20 mL/min). The samples were heated from 50 to 650 °C at a heating rate of 20 °C/ min. The compressive mechanical tests have been conducted according to ASTM-D695M-91 specifications using an Instron universal testing machine (model 4502) at a cross-head speed of 1 mm/min. The cylindrical specimens were 9.0 mm in diameter and 18.0 mm in length. Five specimens were tested for each sample. The compressive strengths correspond to the stress at which the cylindrical specimen breaks.

RESULTS AND DISCUSSION

Chemical Composition of the Bio-based Rubbers

Rubbery transparent polymers have been produced by the free radical copolymerization of highly reactive tung oil and the chemically modified soybean oil called Ebecryl 860. Various mixtures of the two vegetable oils have been screened; all of them have produced rubbery materials. The nomenclature adopted in this work is as follows; a polymer sample prepared from 50 wt % TUNG, 50 wt % EBE, and 1 wt % TBPA is designated as TUNG50/EBE50/TBPA1. As the amount of tung oil increases in the composition of the samples, the material obtained becomes increasingly softer, indicating that the Ebecryl

860 is more prone to form crosslinks that make the materials stiffer. As represented in Figure 1, tung oil contains a large number of carbon-carbon double bonds, which are naturally conjugated; these are the reactive sites that provide the crosslinks from which the polymer forms. On the other hand, Ebecryl 860 does not have conjugated double bonds, but has acrylate moieties that exhibit high reactivity towards free radical polymerization, apparently even greater reactivity than tung oil. This is why as the amount of Ebecryl 860 increases in the composition of the samples the materials become less rubbery and behave more like a hard plastic.

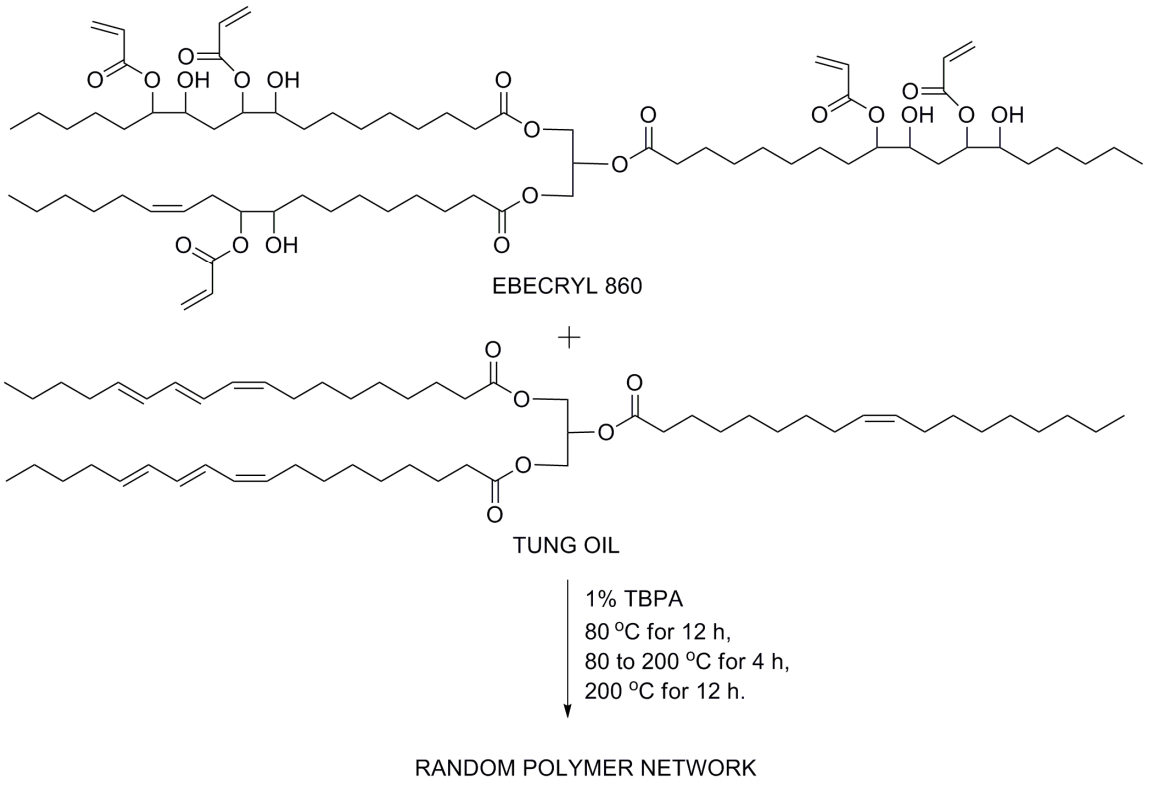

FIGURE 1. Synthesis of the bio-based rubbers.

Dynamical mechanical properties of the bio-based rubbers

The thermal and mechanical properties of these new bio-based rubbers have been examined as the ratio of the two triglyceride oils has been varied. The range of tan delta values obtained for these materials is ~0.3 to ~1.0 as summarized in Table 1, suggesting that these materials can be used for damping sound or vibrations in general, since tan delta values above 0.3 are considered good damping materials [16]. Rubbery materials tend to exhibit higher tan delta values compared with hard plastics, because the flexible links that form the network are better able to spread the vibrations throughout the material and, therefore, are more efficient in the dissipation of these vibrations as heat.

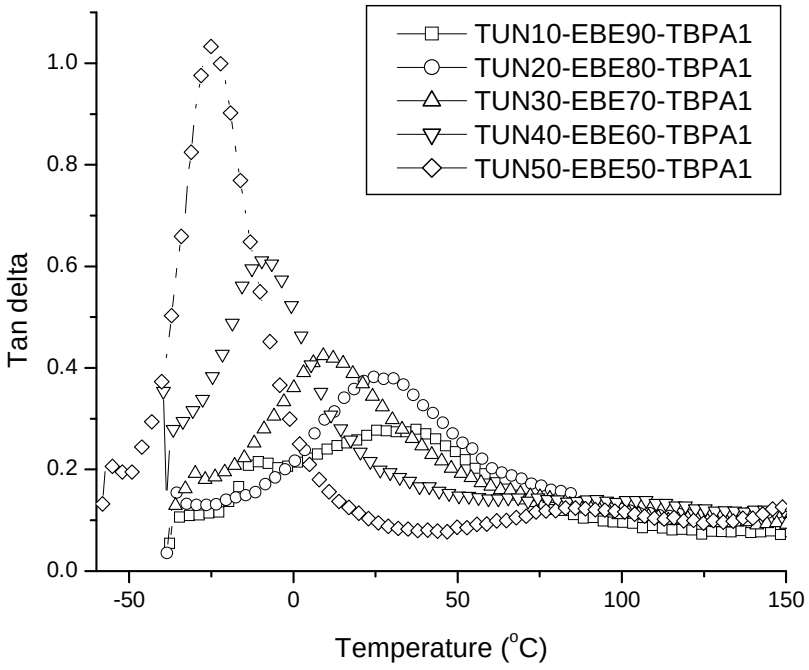

FIGURE 2. Tan delta Curves for the Tung Oil-based Rubbers.

Using a 3 point-bending mode for the dynamic mechanical analysis of these bio-based rubbers, the T_gs of the materials have been found to vary from 27.3 °C to -24.1 °C

(see Table 1). The lower T_g values correspond to samples with a higher tung oil content. This again supports the observation that the Ebecryl 860 is capable of forming more crosslinks. Table 1 also presents the crosslink densities calculated from the storage modulus curves at 40 ^{o}C above the T_g and based on the kinetic theory of rubber elasticity [17]. The values again appear to be lower at higher tung oil content, supporting further our previous explanation. We were able to collect data for only 5 samples containing the higher amounts of Ebecryl 860, since as the amount of tung oil increased in the composition, the samples became softer, and it became impossible to obtain samples suitable for DMA analysis. Therefore, the results obtained from the softer samples became meaningless.

TABLE 1. Dynamic Mechanical Analysis of the Tung Oil/ Ebecryl 860 Samples.

Sample	*Tg* (^{o}C)	Tan Delta	Storage Modulus (MPa)	Loss Modulus (MPa)	Crosslink Density (mol/m^3)
TUNG10/EBE90/TBPA1	27.3	0.28	59.3	16.6	2893
TUNG20/EBE80/TBPA1	24.5	0.38	71.7	27.4	2888
TUNG30/EBE70/TBPA1	9.1	0.42	37.5	15.9	1484
TUNG40/EBE60/TBPA1	-7.6	0.62	18.7	11.5	616
TUNG50/EBE50/TBPA1	-24.1	1.04	6.1	6.3	134

Thermogravimetric and extraction analyses of the bio-based rubbers

Table 2 contains data from the TGA analyses. The temperatures at which the materials lose 10% of their original mass (T_{10}) range between 375 and 420 ^{o}C, and the temperature range for 50% mass loss (T_{50}) is between 445 and 485 ^{o}C. These 100% bio-based rubbery materials are quite thermally stable even at temperatures as high as 350 ^{o}C, indicating that the crosslinks formed between the triglycerides are quite strong, requiring high input of energy in order to break them. The residue in all of these analyses was a flakey-dark char with a mass below 5% of the original mass. All of the samples exhibit a three stage degradation pattern (see Figure 3). All of the samples follow the same behavior with the exception of a few changes in the temperatures at which the degradation events start for the different sample compositions. The temperature of maximum degradation (T_{max}) tends to increase slightly as the amount of tung oil increases in the samples, indicating that the presence of higher concentrations of this naturally conjugated vegetable oil impart some thermal stability to the polymer network, even though the tung oil is not completely incorporated into the polymer network.

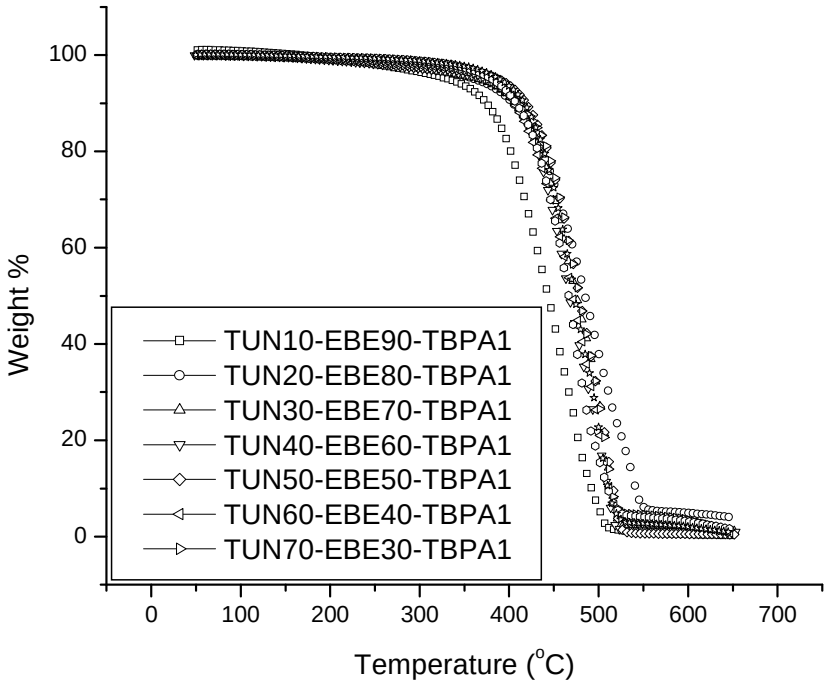

FIGURE 3. TGA Curves for theTung Oil-based Rubbers.

Table 2 also presents data from the Soxhlet extraction analysis. The percent of soluble materials increases as the amount of tung oil increases in the overall composition. The minimum values are around 6% and the higher values range up to 50%, indicating that half of the material is not chemically incorporated into the polymeric network, but this unreacted portion acts as a plasticizer, since the softer, more rubbery materials are the ones with more tung oil in the original mixture.

TABLE 2. Thermogravimetric and Soxhlet Extraction Analysis of the Tung Oil / Ebecryl 860 Samples.

	TGA				Extraction Analysis	
Sample Composition	T_{10} (°C)	T_{50} (°C)	T_{max} (°C)	T_{10}-T_{50} interval (°C)	Sol % ± 3 %	Insol % ± 3 %
TUNG10/EBE90/TBPA1	375	444	474	69	10	90
TUNG20/EBE80/TBPA1	405	485	499	80	7	93
TUNG30/EBE70/TBPA1	407	475	508	68	6	94
TUNG40/EBE60/TBPA1	406	466	500	60	15	85
TUNG50/EBE50/TBPA1	419	479	519	60	25	75
TUNG60/EBE40/TBPA1	405	471	505	66	44	56
TUNG70/EBE30/TBPA1	409	478	511	69	54	46

^{1}H NMR spectroscopic analysis of the vegetable oils and their soluble rubber extracts

The ^{1}H NMR spectra of pure tung oil and Ebecryl 860 are shown in Figures 4 and 5 respectively. The signals for the hydrogens present on the conjugated double bonds of the tung oil appear between 5.0 and 6.5 ppm, roughly the same range where the acrylate hydrogens appear for the Ebecryl 860 (see Figure 5). This overlap of signals makes it impossible to differentiate the oils in the ^{1}H NMR spectra of the extracted portions of

these materials. Even though the true identity of the peaks is hard to decipher, we suspect that most of the extracted materials correspond to tung oil and oligomers, since the amount of such extracts increase as the amount of tung oil in the original composition increases. A signal attributed to the presence of the hydroxyl group of the Ebecryl 860 was also hard to pinpoint among the other signals, making it impossible to confirm the presence of Ebecryl 860 in the extracts.

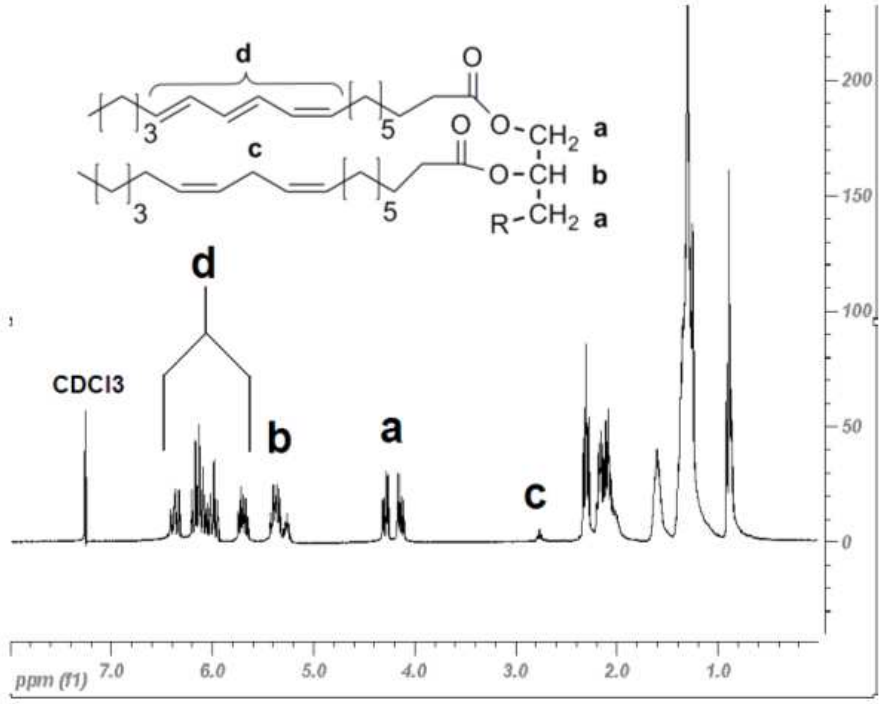

FIGURE 4 ^{1}H NMR Spectrum of Tung Oil.

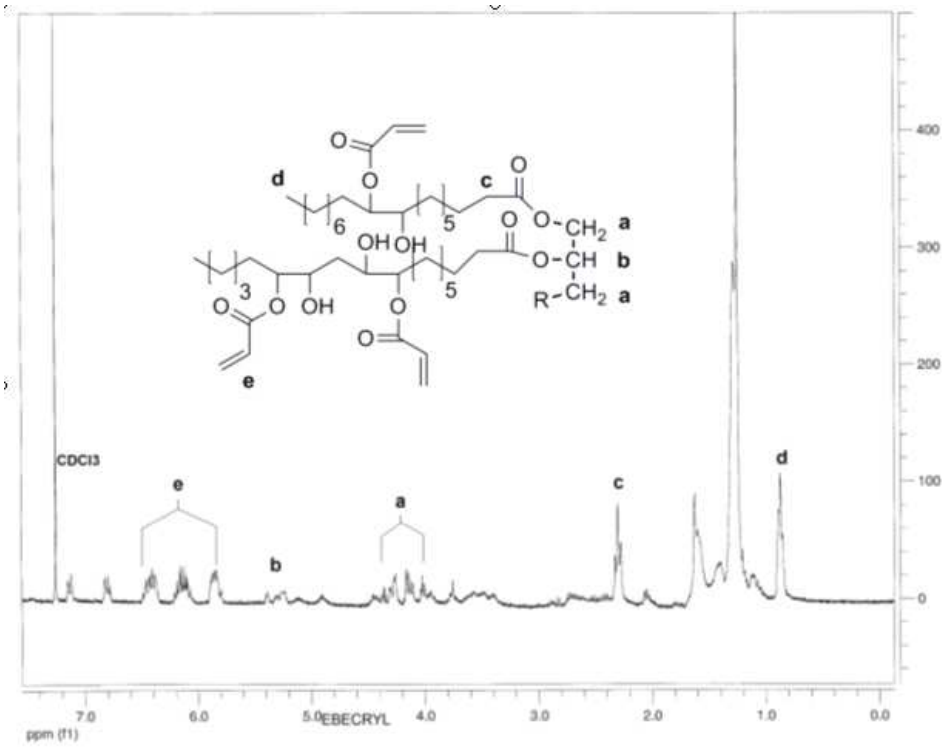

FIGURE 5. ^{1}H NMR Spectrum of Ebecryl 860.

Compression stress-strain performance of the bio-based rubbers

TABLE 3. Compression Analysis of Samples Containing Pure Resin Only.

Sample composition (wt %)	Stress (MPa)	Strain (%)
TUNG10/EBE90/TBPA1	86 ± 5	46 ± 2
TUNG20/EBE80/TBPA1	61 ± 6	47 ± 1
TUNG30/EBE70/TBPA1	23 ± 3	42 ± 3
TUNG40/EBE60/TBPA1	3.7 ± 0.3	39 ± 5
TUNG50/EBE50/TBPA1	2 ± 1	31 ± 1
TUNG60/EBE40/TBPA1	2 ± 1	25 ± 2

In order to better understand the mechanical properties of these new bio-based materials, a more complete study was needed. For that purpose, a compression analysis utilizing cylindrical samples with a 2:1 height to diameter ratio was carried out on an Instron universal mechanical tester. The specifics of such testing are explained in the experimental section of this article.

Figure 6 shows the results from the compression analysis performed on the samples; the stress and strain values are summarized in Table 3. It is evident that there is a significant decrease in stress and strain as the amount of tung oil increases in the composition. The observed diminution does not obey a linear behavior that could be easily attributed to an increase in the concentration of the tung oil or a corresponding decrease in the amount of acrylated monomer Ebecryl 860. This effect might be due to the lack of reactive enough double bonds in the tung oil capable of crosslinking the material and making the resulting rubbers much tougher. Another reason might be that as the amount of tung oil increases in the matrix, the amount of unreacted fatty acid side chains increases, and, as mentioned previously, the major effect of these unreacted chains is plasticization of the polymer matrices by increasing the free volume between the chains, and therefore their mobility. Unfortunately, with this also comes a decrease in the strength and hardness of the materials, which is reflected in the lower stress and strain values observed.

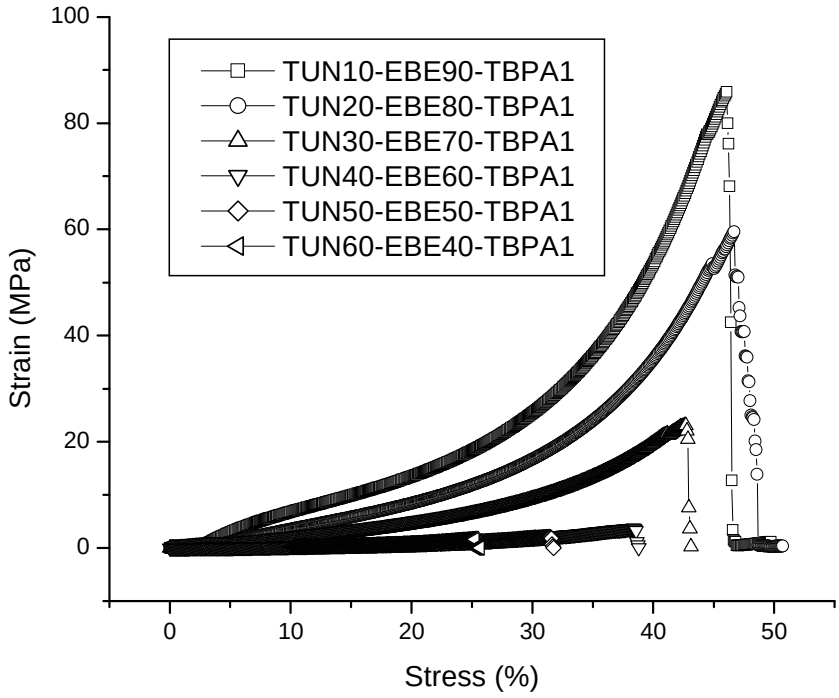

FIGURE 6. Stress-Strain Curves for Pure Resin Samples.

CONCLUSIONS

All of the materials prepared appear promising from an environmental point of view. These rubbery materials have been synthesized entirely from readily available, bio-renewable vegetable oils, and they do not require the addition of petroleum-based comonomers, plasticizers, and/or crosslinkers. Only one of the comonomers has been chemically modified to enhance its reactivity; the other, tung oil, has been used as it is produced in nature, so it requires less overall input of energy. Incorporation of the oils varies from 6 to 50 wt %; the higher percentages correspond to higher amounts of tung oil in the original composition. Any residual unreacted tung oil acts as a plasticizer, increasing the tan delta values, which increase vibrational damping, and it also decreases

the T_gs from ~27 ^{o}C to -25 ^{o}C, providing a wide range of temperatures where these materials behave as rubbers.

A disadvantage of these materials is that they do not show great stress and strain values, which limits their applicability. This problem might be solved by adding additional reinforcement fillers, such as carbon black. This study is currently underway.

ACKNOWLEDGEMENTS

We would like to acknowledge Archer Daniels Midland (ADM) for supplying the tung oil, as well as the George Washington Carver Internship Program at Iowa State University, the Illinois-Missouri Biotechnology Alliance, and the Grow Iowa Values Fund for financial support of this project.

REFERENCES

[1] Bisio AL, Xanthos M. How to Manage Plastics Wastes: Technology and Market Opportunities. New York: Hanser Publishers, 1995.

[2] Di Pierro P, Chico B, Villalonga R, Mariniello L, Damiao A, Masi P, Porta P. Biomacromolecules. 2006; 7(3): 744-749.

[3] Mohanty, AK, Liu W, Tummala P, Drzal LT, Misra M, Narayan R. Soy Protein-based Plastics, Blends, and Composites. In: Mohanty,A, Misra M, Drzal L, editors. Natural Fibers, Biopolymers, and Biocomposites. Boca Raton: Taylor & Francis Group, 2005 pp. 699.

[4] Mizobuchi Y. U.S. Patent 5395435; 1995.

[5] Bonacini V. European Patent Office, WO 02/44490 A1; 2002.

[6] Li F, Hanson MV, Larock RC. Polymer 2001; 42(4): 1567-1579.

[7] Formo MW. In: Swern D editor. Bailey's Industrial Oil and Fat Products, vol. 2. 4th ed. New York: Wiley, 1982, pp 343-405.

[8] Li F, Larock RC. J. Appl. Polym. Sci. 2000; 78(5): 1044-1056.

[9] Valverde M, Andjelkovic DD, Kundu PP, Larock RC. J. Appl. Polym. Sci. 2007; 107(1): 423-430.

[10] Williams GI, Wool RP. Appl. Comp. Mat. 2000; 7(5-6): 421-432.

[11] Li F, Larock RC. Biomacromolecules 2003; 4(4): 1018-1025.

[12] Li F, Larock RC. Synthesis, Properties, and Potential Applications of Novel Thermosetting Biopolymers from Soybean and Other Natural Oils. In: Mohanty A, Misra M, Drzal L, editors. Natural Fibers, Biopolymers, and Biocomposites. Boca Raton: Taylor & Francis Group, 2005 pp. 727.

[13] Kundu PP, Larock RC. Biomacromolecules 2005; 6(2): 797-806.

[14] Khot SN, Lascala JJ, Can E, Morye SS, Williams GI, Palmese GR, Kusefoglu SH, Wool RP. J. Appl. Polym. Sci. 2001; 82(3): 703-723.

[15] Billmeyer FW. Textbook of Polymer Science, 2nd ed. New York: Wiley-Interscience, 1971, pp. 282-283.

[16] Nielsen LE, Landel RF. Mechanical Properties of Polymers and Composites, 2nd ed. New York: Marcel Dekker, 1994.

[17] Andjelkovic DD, Valverde M, Henna P, Li, F, Larock RC. Polymer 2005; 46(23): 9674-9685.

CHAPTER 4. CONJUGATED SOYBEAN OIL-BASED RUBBERS: SYNTHESIS AND CHARACTERIZATION

A Paper to be Published in Macromolecular Materials and Engineering

Marlen Valverde,[1] Sungho Yoon,[2,4] Satyam Bhuyan,[3] Richard C. Larock,[1*] Michael R. Kessler,[2] Sriram Sundararajan[3]

[1] Department of Chemistry, [2] Department of Materials Science and Engineering, [3]Department of Mechanical Engineering, Iowa State University, Ames, IA
[4] School of Mechanical Engineering, Kumoh National Institute of Technology, Yangho-Dong, Gumi, Gyeongbuk, 730-701, Korea

Abstract

A range of bio-based rubbery thermosets have been synthesized by the cationic copolymerization of conjugated soybean oil, styrene, 1,5-hexadiene or isoprene and SoyGold® using boron trifluoride diethyl etherate as the initiator. The thermal, and mechanical properties, as well as the wear behavior, of these new bio-rubbers are reported. The amount of styrene and the type of diene incorporated have the greatest influence on the properties of the final materials. The largest variations are found in glass transition temperature, storage modulus, tan δ values, crosslink density, and abrasive wear depth, while thermal degradation and extraction analyses showed minimal variations with changes in composition.

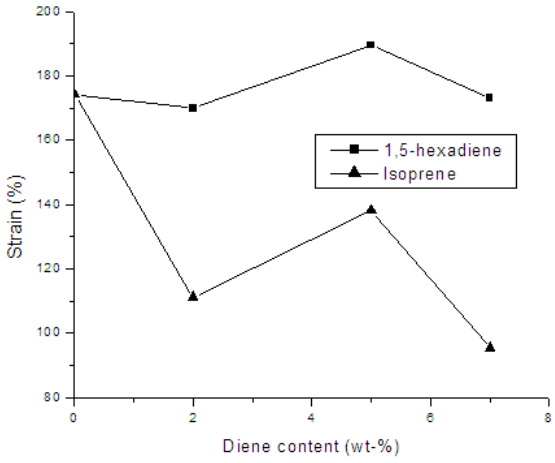

Introduction

Numerous problems arise from the use of petroleum-based substances in the synthesis of polymeric materials. Among the most important and evident problems are (1) the source of petroleum is finite, (2) extraction of petroleum is a costly activity, which can also generate extreme contamination, (3) the price of oil is subject to sharp fluctuations linked to the world economy and politics,[1] and (4) degradation of petroleum-based materials is normally a lengthy process that generates toxic molecules that many endanger life and ecosystems.[2] Over all, the continuous use of petroleum is not a "green" or sustainable activity.

Bio-based materials in general have been catching the scientific community's attention for the past decade as viable candidates to replace in total or in part many resins,[3] hard polymers, paints, adhesives, and rubbers that come mostly from petroleum.[4-6] The biggest challenge in using bio-based sustainable materials in polymer synthesis is their relatively low reactivity,[7] which requires the incorporation of functional groups that will allow better chemical incorporation into the polymeric network. The reaction conditions used to modify these materials have to be gentle enough to prevent premature decomposition or loss of biodegradability.[8]

Many research groups have been successful in incorporating bio-based monomers into materials that range from drug delivery systems[9] to zero volatile organic compounds (VOC)-containing paints.[10] We have had success in synthesizing thermoset polymers and composites, whose main starting material is a vegetable oil or a combination of oils.[11-14] These polymers range from soft and rubbery to hard and brittle for a broad range of potential uses.[13] Recently, novel new waterborne polyurethanes

have been developed from natural oil derivatives with exceptional performance as clear coatings and possible adhesives.[15]

Vegetable oil triglycerides are biodegradable and also very versatile monomers, since they can polymerize through the carbon-carbon double bonds present in their long aliphatic chains via various polymerization techniques, including cationic,[5] free radical,[16] thermal,[17] ring opening metathesis,[18-19] and emulsion polymerization.[20] Functionalization of the double bonds is also possible, allowing one to transform the fatty acid side chains into epoxide-, alcohol-, urethane-,[15] or acrylic-[21] containing side chains. These functionalized chains can react by many different routes to give rise to polymeric networks with special thermal and mechanical characteristics.

Functionalization of the carbon-carbon double bonds has the down side that this increases the price of the oil significantly. Thus, it is preferable to synthesize bio-based polymers directly from vegetable oils. Working with unmodified vegetable oils requires the use of other comonomers that have a reactivity similar to that of the oil or help to better incorporate the oil into the polymeric network. In the past, we have used several different comonomers in low amounts because the majority of which are petroleum-based for this purpose.[16] We have also observed that when a high loading of vegetable oil is present in the bio-based polymers, soft and rubbery materials can be synthesized.[21]

Andjelkovic and co-workers thoroughly screened a system comprised of different types of soybean oil and styrene (ST).[22] They found that samples containing large amounts of regular (SOY) or conjugated soybean oil (CSOY) were rubbery and had a relative high elongation at break.[22] The better chemical incorporation of the CSOY molecules into the polymer network imparts softness to the materials. The reason CSOY

is incorporated better into the network is because the conjugated C=C bonds (averaging 4.6 per triglyceride unit) are more reactive towards cationic polymerization, since allylic carbocations are formed upon attack of the activated species.[22]

Natural rubber or latex,[23] polycaprolactone,[24] and polyhydroxybutyrate[25] have been used as replacements for petroleum-based comonomers in the fabrication of different types of rubber, most of them being used in greener passenger vehicle tires.[26] Oil palm fiber has been used as a natural filler in such materials.[23] Despite all of these efforts, none of these "green" rubbers incorporate large loads of a renewable and readily available resource, like a vegetable oil.

The tribological (friction and wear) properties of biobased polymers made from CSOY copolymerized with ST and divinylbenzene (DVB) monomers have been studied by Bhuyan *et. al*[27,28] as a function of their crosslinking densities. It has been found that materials with higher crosslinking densities show improvement in friction and wear behavior.

In this work, we wish to report our most recent bio-based rubbers prepared by the cationic copolymerization of CSOY, ST, 1,5-hexadiene (HEX) or isoprene (ISO) as flexible crosslinkers, and a mixture of soybean oil methyl esters, known as SoyGold ®1100 (SG), as a plasticizer. The synthesis, structure, and thermal and mechanical properties of these new materials are presented in this paper.

Experimental Part

Materials

The soybean oil used in this study is a food-grade oil purchased in the local supermarket. The CSOY was prepared by the rhodium-catalyzed isomerization of the soybean oil.[22] The percent conjugation is calculated to be approximately 100%. The ST comonomer, HEX and ISO crosslinkers, and boron trifluoride diethyl etherate (BFE) used as the cationic initiator were purchased from Aldrich Chemical Company and used as received. The SoyGold® 1100 (SG) was generously supplied by Ag Environmental L.L.C. from Omaha, NE, and used as received.

Polymer Preparation and Nomenclature

Varying amounts of CSOY, ST, HEX or ISO, SG, and BFE were mixed in a rectangular glass mold built with two glass plates 20 cm long by 15 cm wide. The two plates covered with a thin sheet of PE-*co*-Teflon releasing film were separated by a rubber gasket 0.3 cm wide and held together by 8 metal spring clamps. The amount of CSOY oil was varied from 40 to 60 wt-%. The glass molds were maintained at room temperature for the first 12 h and then heated at 60 °C for 12 h, and finally at 110 °C for 24 h. The nomenclature adopted in this work for the polymer samples is as follows: a polymer sample prepared from 40 wt-% CSOY, 42 wt-% ST, 5 wt-% ISO, 5 wt-% SG, and 3 wt-% BFE is designated as CSOY40/ST42/ISO5/SG5/BFE3.

Testing

Soxhlet Extraction. A 2 g sample of the bulk polymer was extracted for 24 h with 100 mL of refluxing methylene chloride using a Soxhlet extractor, and the resulting solution was concentrated by rotary evaporation and subsequent vacuum drying. The soluble substances were characterized further by ^{1}H NMR spectroscopy.

^{1}H NMR Spectroscopic Characterization. The ^{1}H NMR spectra of the extracted soluble substances were obtained in $CDCl_3$ using a Varian Unity spectrometer at 300 MHz.

Dynamic Mechanical Analysis (DMA). The DMA experiments were performed using a model Q800 dynamic mechanical analyzer (TA Instruments) in tensile mode. Rectangular specimens obtained from the molded sheets had dimensions of 2 × 4 × 30 mm ($t \times w \times l$). Each specimen was installed in a tensile fixture to align the longitudinal axis of the specimen with the loading line. The specimen was first cooled to -120 °C and then heated to 80 °C at a heating rate of 3 °C/min. All measurements were conducted using an amplitude of 5.0 μm, a frequency of 1 Hz, a static force of 0.02 N and a force track of 130%. The storage moduli and tan δ values were recorded as a function of temperature. The glass transition temperatures (T_g) of the samples were measured from the peaks of the tan δ curves.

Thermogravimetric Analysis (TGA). The thermogravimetric analyses were performed on a model Q50 TGA Instrument (TA Instruments). The sample was equilibrated at 30 °C for 1 minute isothermally and then heated to 700 °C at a heating rate of 20 °C/min in air. The weight loss as a function of temperature was measured.

Tensile Tests. The tensile properties of the bio-based rubbers were determined by using a universal material testing system (model 4502, Instron). All specimens were obtained

using a punch-type cutter from the molded sheets described above. A specimen configuration having a gauge section of 50 mm, a width of 10 mm, and a thickness of 3 mm was adopted consistent with an ASTM D638 type V specimen. The tensile tests were conducted at an ambient temperature and a crosshead speed of 5 mm/min, while specimen strain was measured using a video extensometer. The tensile modulus was calculated from the initial slope of the tensile stress-strain curve in a strain range of 1 to 10 %. The tensile strength was determined from the load at fracture and the failure strain from the strain at fracture.

Wear Analysis. For the experiments described in this paper, a custom-built reciprocating ball-on-flat microtribometer that can produce a microscale (apparent area ~1000 square microns) multi-asperity contact was used.[29] All samples were subjected to 100 cycle reciprocating dry sliding wear tests against a sharp diamond probe (100 micron radius, 90° cone angle) at a constant normal load 100 mN and a sliding speed of 5 mm/s. Preliminary tests showed that, for the given load conditions, the sliding speed had a negligible effect on the wear relative to other factors. All tests were performed at 24 ^{o}C and 30 ± 2 % relative humidity. Three trials were carried out on a single batch of samples. Wear track profiling was carried out using a contact profilometer (Dektak II).

Scanning Electron Microscopy (SEM). High resolution images of the wear tracks on the probes were obtained using a JOEL JSM-6060LV Scanning Electron Microscope. Five readings from each trial were taken and the average and standard deviation of the wear depth from all three trials have been reported.

Results and Discussion

Scheme 1 is a representation of a generic bio-based rubber made by cationic polymerization with ST as the comonomer, SG as the primary plastisizer, and ISO as the crosslinker. These materials are thermosets with a high degree of elasticity, which depends largely on the load and type of diene. The resulting materials are dark brown in color with a glossy surface, and almost odorless. During the synthesis, we initially observed the presence of some voids in the materials produced by bubbles formed during the heating processes. This problem was solved by very slowly heating the materials to prevent sudden void formation.

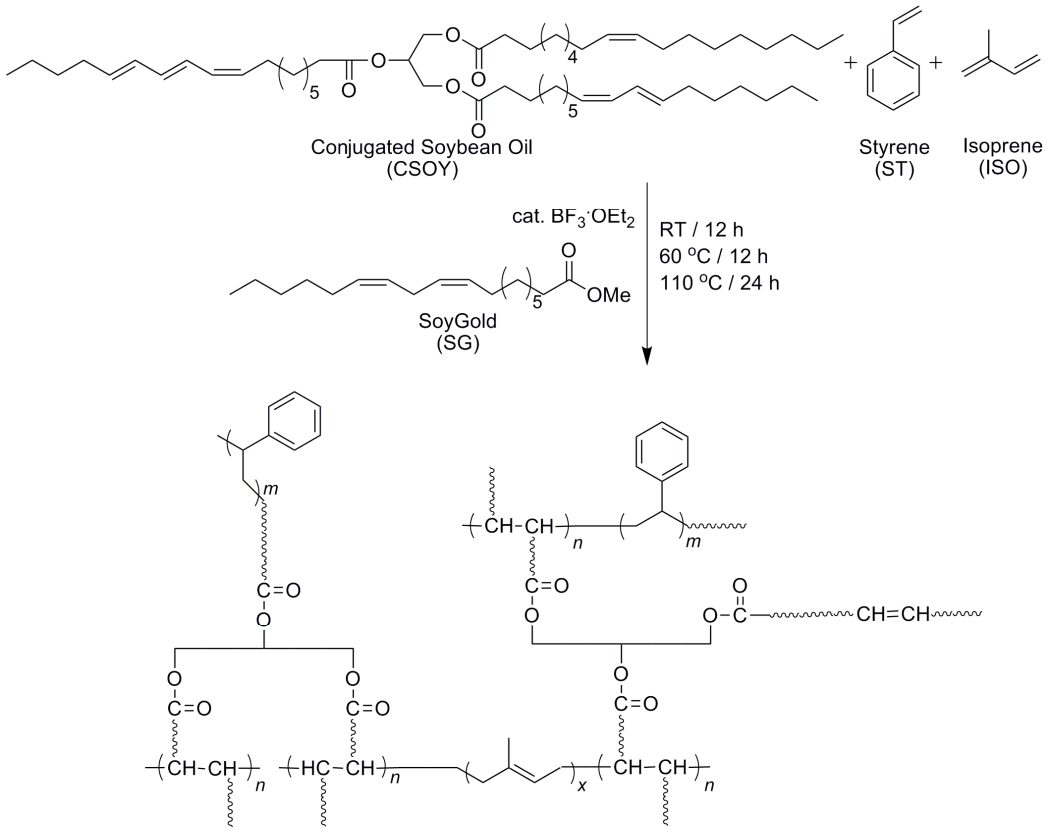

Scheme 1. Synthesis of the bio-based rubbers containing ISO.

Table 1. Dynamic Mechanical Analysis of the Bio-based Rubbers.

Sample Composition	*Tg* (°C)	Tan δ	Storage Modulus (MPa)	Loss Modulus (MPa)	Crosslink Density (mol/m^3)
1,5-Hexadiene					
CSOY45/ST47/HEX0/SG5/BFE3	24.8	1.68	4.7	7.9	28
CSOY45/ST45/HEX2/SG5/BFE3	21.1	1.69	4.4	7.4	24
CSOY45/ST42/HEX5/SG5/BFE3	18.3	1.79	3.5	6.3	15
CSOY45/ST40/HEX7/SG5/BFE3	16.1	1.82	3.3	6.0	11
CSOY55/ST35/HEX7/SG0/BFE3	14.1	1.60	5.7	9.1	41
CSOY60/ST35/HEX2/SG0/BFE3	11.3	1.44	7.7	11.2	65
Isoprene					
CSOY45/ST45/ISO2/SG5/BFE3	19.9	1.69	4.6	7.8	34
CSOY45/ST42/ISO5/SG5/BFE3	17.8	1.75	5.2	9.1	40
CSOY45/ST40/ISO7/SG5/BFE3	20.2	1.74	5.8	10.1	44
CSOY55/ST35/ISO7/SG0/BFE3	20.2	1.55	7.4	11.5	87
CSOY60/ST35/ISO2/SG0/BFE3	14.0	1.36	7.5	10.3	89

Table 1 summarizes the DMA values found for these bio-based rubbers. It is observed that the T_g decreases for the system containing HEX as the amount of HEX increases and the amount of ST decreases. See Figure 1(a). This effect is expected when decreasing the ST content, since ST has the ability to develop π–π stacking interaction that introduces rigidity to the polymer chains and ultimately increases the T_g. Decreasing the amount of ST should, therefore, be reflected in a lowering of the glass transition temperature. ISO-containing samples initially exhibit the same trend shown by the HEX-containing samples for ISO loadings up to 5 wt-%. Their T_g values decrease with increasing ISO concentration and decreasing ST content, but the effect in this case is not as pronounced as it is in the HEX system. In addition, the T_g increases slightly at 7 wt-%

ISO. In addition the T_g increases slightly at 7 wt-%. See Figure 1(b). Perhaps this is because the ISO is more readily incorporated into the polymeric chains, since they do not seem to loose as much stiffness as in the case of the HEX-containing samples. The reason for this could be that HEX has only two terminal double bonds that are not in conjugation. Their reactivity towards cationic polymerization is therefore lower than that of ISO.

The storage modulus tends to decrease as the concentration of ST decreases in the HEX system. The lower values may be a result of the lack of polystyrene-rich segments in the bio-rubber. These polystyrene segments have the ability to develop π–π stacking as stated before. This ultimately imparts higher rigidity to the materials. When they are not present, one expects to see a decrease in the values of certain mechanical characteristics, like *E'*, and parameters derived from *E'*, such as the crosslink density. On the other hand, higher incorporation of HEX imparts flexibility to the polymer chains of the materials due to the four carbons between the two double bonds. These factors work in concert to give a lower *E'*; see Figure 1(a). In the case of ISO, we see the opposite effect (see Figure 1(b)). Here the *E'* increases as the amount of ISO increases. This increase may be due to the fact that synthetic polyisoprene-containing materials are known to have unexpectedly high storage moduli due to the relatively high number of crystalline domains that can form during polymerization. *trans*-polyisoprene present in high quantities in synthetic polyisoprene has this tendency.[30, 31]

In order to have a rapid and completely reversible deformation in a material, the material needs to have some degree of crosslinking. Dienes can be used as monomers that form these crosslinks during copolymerization, which involves mostly, but not

exclusively, the formation of linear polymer chains.[30] The formation of crosslinks may happen at different stages during the polymerization, depending on the reactivity of the double bonds of the dienes, and the amount of crosslinks formed, which also depends on the relative amounts of the diene and the other monomers present in the composition.[30] The crosslink densities of the CSOY rubbers seem to follow the same trend exhibited by the storage moduli. The values decrease for the HEX-containing samples [see Figure 1(a)], but the opposite is observed for the ISO-containing samples [see Figure 1(b)]. In order to calculate the crosslink density of a thermosetting material, we have utilized equation 1, where υ_e is the crosslink density and R is the gas constant in SI units, which is derived from rubber elasticity theory and utilizes the value of the storage modulus at 40 ^{o}C above the T_g. If the material has a low *E'* value above the T_g, its crosslink density will be a low value as well.[32]

$$\upsilon_e = \frac{E'}{3RT} \qquad (1)$$

The ratio of *E"* to *E'* or the tan δ values of all the samples were taken at the T_g and range from 1.36 to 1.82, indicating that these materials, in general, possess a high damping ability. The sample that does not have any diene has the lowest of all the values, indicating that both dienes impart better damping ability to the polymeric networks [see Figure 1(c) and (d)]. In both cases, samples containing HEX and ISO show an increase in tan δ values as the amount of the diene increases. For the ISO samples, this increase is not as pronounced. It is also worth noting that the increasing tan δ values are accompanied by decreasing storage modili, loss moduli, and crosslink densities.

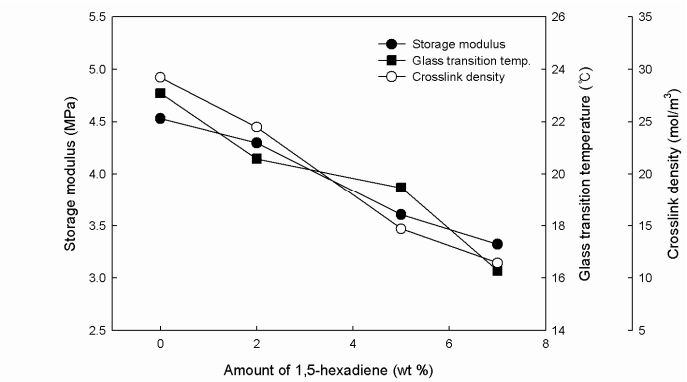

(a) Variation in storage modulus, T_g, and crosslink density with HEX

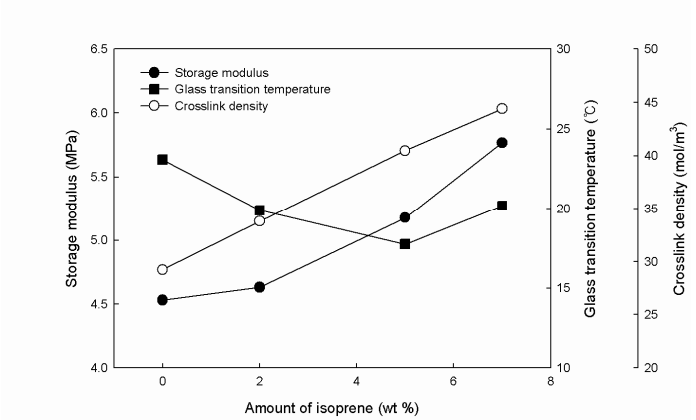

(b) Variation in storage modulus, T_g and crosslink density with ISO

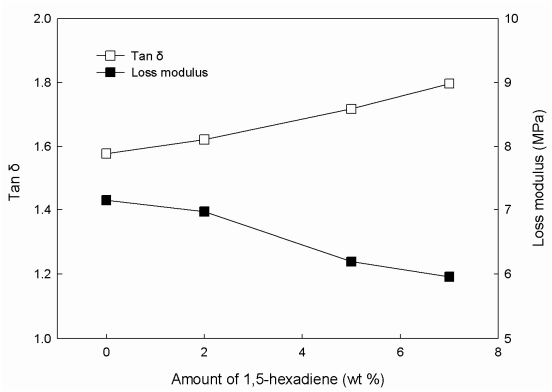

(c) Variation in tan δ and loss modulus with HEX

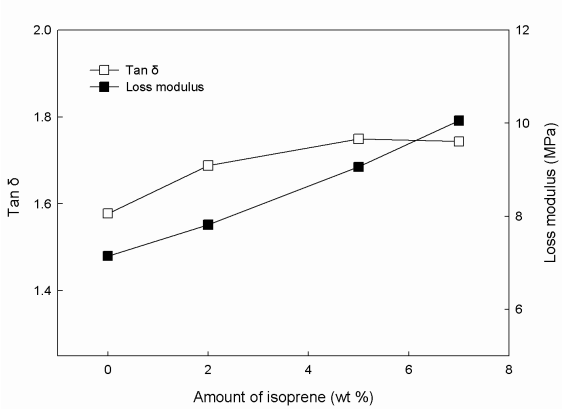

(d) Variation in tan δ and loss modulus with ISO

Figure 1. Variation in the thermomechanical properties for bio-based rubbers with different amounts of diene.

Another interesting aspect of these bio-rubbers is the effect of omitting the SG plasticizer. SG is a mixture of methyl esters from soybean oil, some of these unsaturated fatty acid ester chains may react with the cationic initiator, but they do not have the ability to form crosslinks that will stiffen the material and therefore increase the T_g, crosslink density, *E'*, and *E"*. From Table 1, we can see that bio-rubbers containing HEX or ISO, but no SG, show a significant increase in crosslink density compared similar composites without SG. This suggests that the SG predominantly acts as a plasticizer, lowering the *E'* and subsequently the crosslink density. Its absence should therefore result in an increase in *E'*, when comparing equal loads of the respective dienes [see Figure 2(a) for HEX and 3(a) for ISO]. Indeed, omission of the SG leads to stiffer materials capable of withstanding higher loads during analysis.

Samples without SG also show lower T_g values that might be linked to the fact that these samples contain even less ST and more CSOY, which is known to decrease the T_g by the plasticizing effect of the long fatty acid side chains. The decrease in T_g is observed at the peak of the tan δ curve [see Figure 2(b) for HEX and 3(b) for ISO]. In these figures, we can also see that samples without any SG also exhibit lower tan δ values overall, but they still follow the trend that with more diene the values increase. It seems, therefore, that the presence of SG increases the tan δ by acting as a plasticizer. This effect has been studied further elsewhere.[33]

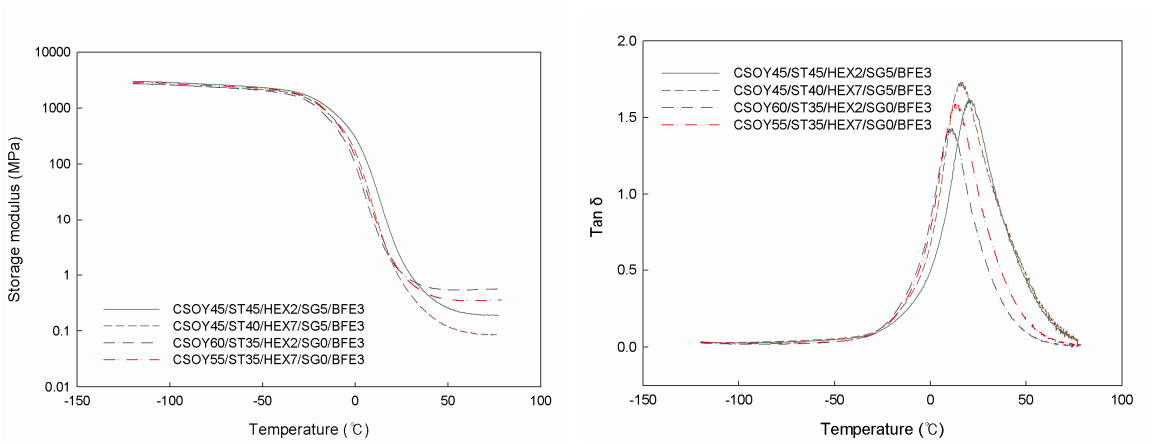

(a) Storage modulus (b) *Tan δ*

Figure 2. DMA results showing the variation in thermomechanical properties for the bio-based HEX-containing rubbers with and without SG.

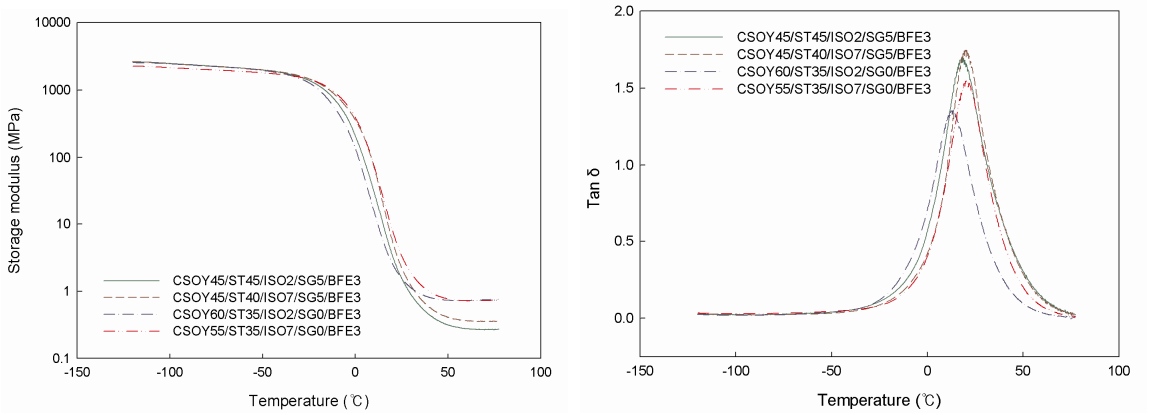

(a) Storage modulus (b) Tan δ

Figure 3. DMA results showing the variation in thermomechanical properties for the bio-based ISO-containing rubbers with and without SG.

Table 2. Thermogravimetric and Soxhlet Extraction Analysis of the Bio-rubbers.

	TGA				Extraction Analysis	
Sample Composition	T_{10} (°C)	T_{50} (°C)	T_{max} (°C)	T_{10}-T_{50} interval (°C)	**Sol (%)**	**Insol (%)**
1,5-Hexadiene						
CSOY45/ST47/HEX0/SG5/BFE3	314	432	431	118	1±1	99±1
CSOY45/ST45/HEX2/SG5/BFE3	305	429	429	124	1±1	99±1
CSOY45/ST42/HEX5/SG5/BFE3	298	424	423	126	2.5±0.3	97.5±0.3
CSOY45/ST40/HEX7/SG5/BFE3	287	427	424	140	4±1	96±1
CSOY55/ST35/HEX7/SG0/BFE3	307	430	430	124	2±1	98±1
CSOY60/ST35/HEX2/SG0/BFE3	314	435	435	121	1±1	99±1
Isoprene						
CSOY45/ST45/ISO2/SG5/BFE3	306	431	431	125	0.3±0.1	99.7±0.1
CSOY45/ST42/ISO5/SG5/BFE3	305	429	425	124	1±1	99±1
CSOY45/ST40/ISO7/SG5/BFE3	304	432	432	128	2.3±0.4	97.7±0.4
CSOY55/ST35/ISO7/SG0/BFE3	315	440	441	125	1.5±0.8	98.5±0.8
CSOY60/ST35/ISO2/SG0/BFE3	312	441	444	129	2±1	98±1

Table 2 summarizes the thermogravimetric and extraction analyses performed on the bio-rubbers. All samples show a very distinct three-stage degradation pattern as seen in Figures 4(a) and 5(a), which presumably arises from early degradation of the unreacted CSOY and possibly SG, when present, followed by thermal decomposition of the bulk polymeric network, and finally decomposition of the char. All of the samples approach 100 % degradation at the maximum temperature of the analysis, which was 700 °C. T_{10} denotes the temperature at which the materials loose 10 % of their original mass. The T_{10} values for all of the samples fall in the same small range of temperatures (278 to 315 °C), regardless of the composition or variations in the comonomer ratios. T_{50}, the temperature at half weight loss, is c.a. 430 °C for all of the samples, roughly the same temperature

values as the T_{max}, the temperature of maximum degradation. The T_{10}-T_{50} interval is therefore very similar for all of the samples. This similarity in the process of thermal degradation and the temperatures for T_{10} and T_{50} is surprising, because one would expect to see a distinct difference in the temperatures when the amount of ST is varied. One reason for this similarity in T_{10} and T_{50} temperatures exhibited by these bio-rubbers could be that when the ST concentration decreases along with an increasing diene concentration, incorporation of the diene compensates structurally for what is lost by the lower ST incorporation.

Extraction analysis for these samples shows a small increase in soluble materials when the amount of diene increases in the original composition. This increase, however, disappears when the error associated with each measurement is taken into account. In this case, all values tend to be very similar and no clear trend is observed. This similarity in the amount of soluble materials is consistent with the explanation given earlier for the similar degradation temperatures. The ^{1}H NMR spectra of the soluble materials indicate that the unreacted material is composed mostly of CSOY and SG, when present. It is very difficult to assign the signals, since most of them overlap and the spectra better matches that of the pure CSOY. It is hard to identify any other comonomer in the NMR spectra.

The presence or absence of SG in the samples does not affect to a large degree the thermal degradation pattern of the samples, nor the rate at which it occurs [see Figures 4(b) and 5(b)]. This indicates that chemical incorporation of the SG into the polymeric networks has little impact on the thermal behavior of the bio-rubbers, although it has a large influence on the mechanical properties.

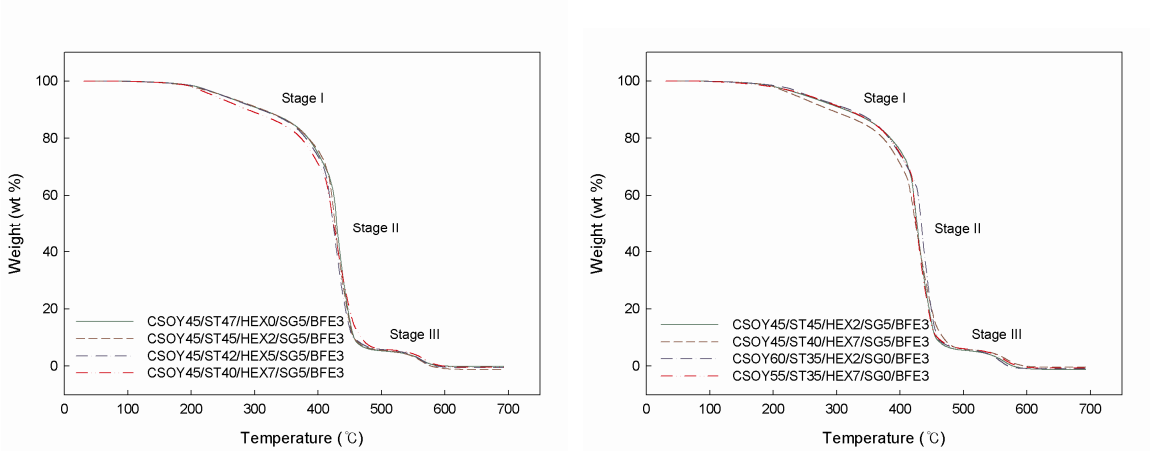

(a) Different amounts of HEX (b) Effect of SG

Figure 4. TGA results showing the variation of weight loss for bio-based rubbers containing HEX.

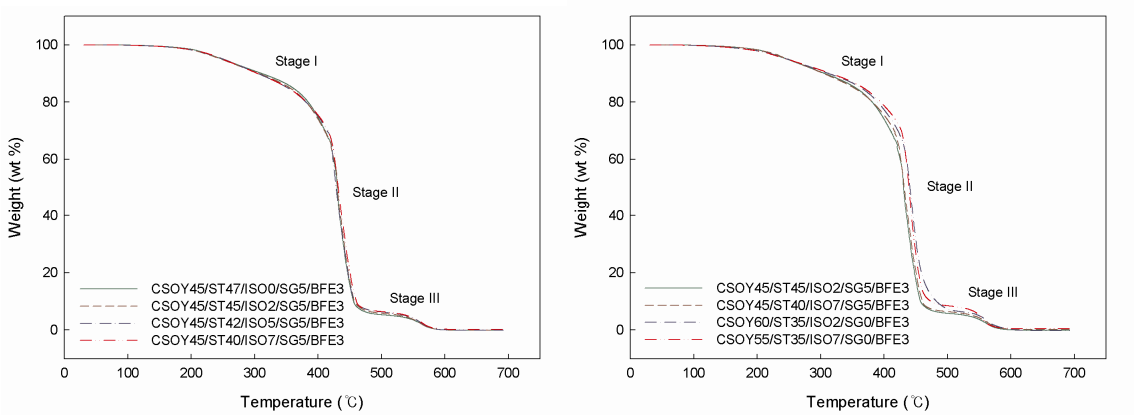

(a) Different amounts of ISO (b) Effect of SG

Figure 5. TGA results showing the variation of weight loss for bio-based rubbers containing ISO.

Table 3. Tensile Analysis of the Bio-based Rubbers.

Sample Composition	Modulus (MPa)	Ultimate Stress (MPa)	Failure Strain (%)
1,5-Hexadiene			
CSOY45/ST47/HEX0/SG5/BFE3	0.206	0.376	174.2
CSOY45/ST47/HEX2/SG5/BFE3	0.159	0.292	169.9
CSOY45/ST42/HEX5/SG5/BFE3	0.096	0.191	189.6
CSOY45/ST40/HEX7/SG5/BFE3	0.064	0.110	173.2
CSOY55/ST35/HEX7/SG0/BFE3	0.261	0.199	88.4
CSOY60/ST35/HEX2/SG0/BFE3	0.414	0.239	66.0
Isoprene			
CSOY45/ST45/ISO2/SG5/BFE3	0.243	0.200	111.3
CSOY45/ST42/ISO5/SG5/BFE3	0.258	0.391	138.2
CSOY45/ST40/ISO7/SG5/BFE3	0.312	0.248	95.5
CSOY55/ST35/ISO7/SG0/BFE3	0.617	0.607	95.5
CSOY60/ST35/ISO2/SG0/BFE3	0.630	0.463	77.9

Tensile analyses have been performed on dog-bone shaped specimens with dimensions dictated by the ASTM D638 type V parameters. The first characteristic to be evaluated was the modulus (MPa), which decreases as the ST concentration decreases and the HEX concentration increases. The reduction of the stiffer polystyrene chains presumably accounts for the significantly lower modulus values. With the materials containing ISO, the opposite trend is observed: the modulus increases with the concentration of ISO. As mentioned before, ISO has the capability of forming crystalline domains which may explain this compensating effect. In all cases, the absence of SG causes the modulus to increase.

The ultimate stress shows the same trend exhibited by the Young's modulus for the HEX-containing samples. A noticeable decrease results when the HEX concentration increases, indicating that this particular diene weakens the bio-rubber significantly. Samples with ISO do not show a clear trend. They do, however, show higher values than the HEX samples.

The ultimate or failure atrains of these rubbers are of particular interest, since this parameter be used to identify the compositions that give materials with elongations approaching synthetic rubbers. Figures 6(a) and 7(a) show typical stress-strain behavior for samples with HEX and ISO respectively. For the HEX samples, we can see that increasing amounts of diene result in a well defined decrease in the ultimate tensile stress, accompanied by a less prominent increase in the tensile strain. On the other hand, ISO-containing samples exhibit increasing failure stress as the amount of ISO increases, but here again the opposite is observed for the tensile strain as an inverse effect arises with higher loads of the diene. Figures 6(b) and 7(b) present a comparison between the samples with and without SG for the HEX and ISO systems respectively. The most obvious effect observed when the SG is omitted is the lower tensile strain values for both systems, accompanied by an increase in the slope of the stress-strain curve (*i.e.* the modulus). These observations can be explained by a true plasticizing effect of the mixture of fatty acid methyl esters of soybean oil. This is, however, the subject of another study presented elsewhere.[33]

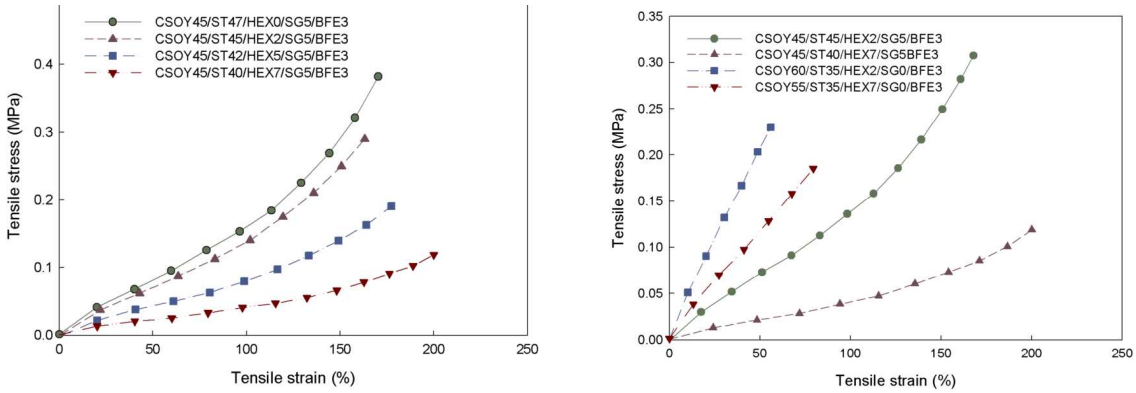

(a) (b)

Figure 6. Tensile test results for CSOY-based bio-rubbers with (a) different amounts of ST and HEX, and (b) different amounts of CSOY, ST, HEX, and SG.

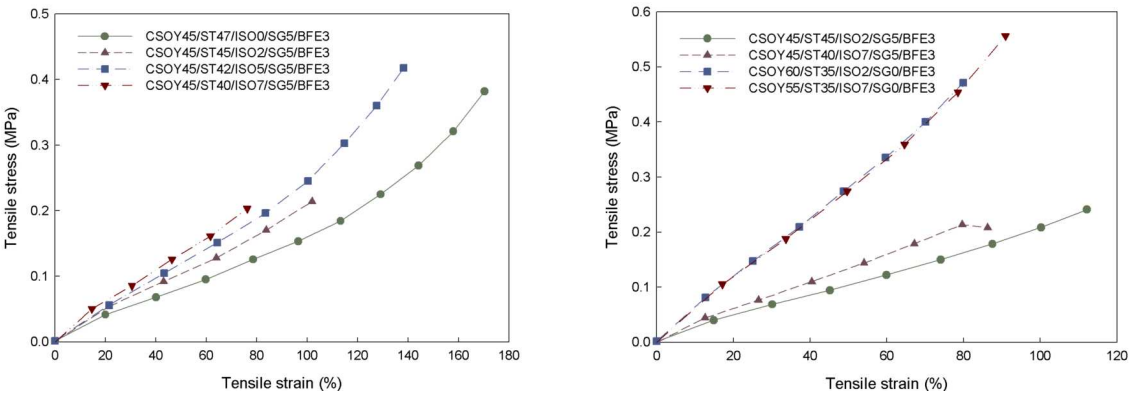

(a) (b)

Figure 7. Typical tensile test results for CSOY-based bio-rubbers with (a) different amounts of ST and ISO, and (b) different amounts of CSOY, ST, ISO, and SG.

Figure 8 illustrates the average wear depths of the samples that have been subjected to a reciprocating wear test with the microtribometer. Clearly the samples with HEX as the crosslinker (1 to 6) show higher wear depth than the ones with ISO (7 to 11).

This indicates that ISO does a better job in resisting wear than HEX. Samples 8 and 10 did not show any wear at all, indicating that these two compositions show resistance to wear under the given load.

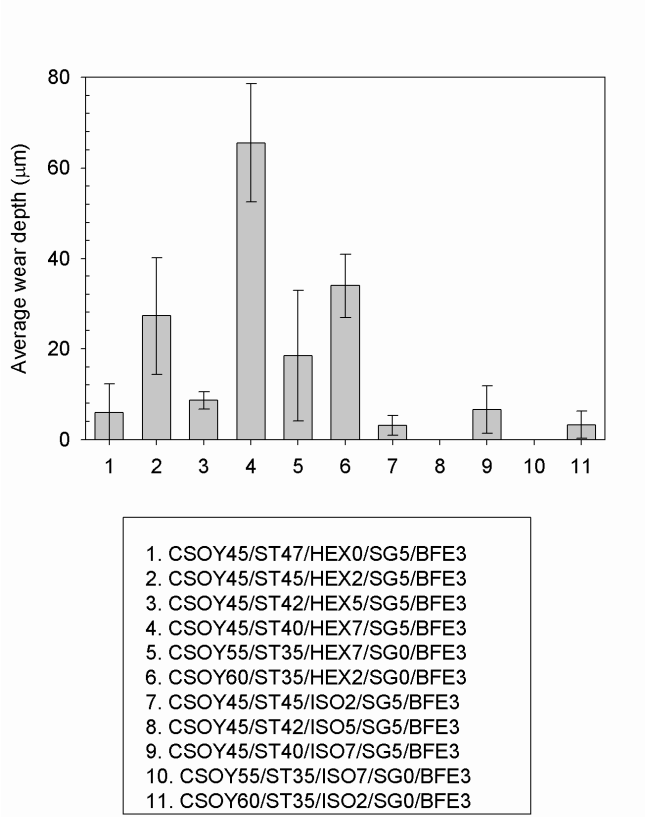

Figure 8. Histogram of the average wear depth of the samples that have been subjected to tests with the microtribometer.

Representative SEM images of samples 4 and 9, which show the highest wear depth for the HEX and ISO samples respectively, are shown in Figure 9. It can be clearly seen that the samples exhibit grooves, as well as the presence of abraded material debris and some cracking along the groove edges. The HEX samples (sample 4 in this case) display a high degree of cracking with negligible debris. Abrasive wear is manifested by

the cutting or plowing of the surface by the harder material (diamond in our experiments). The abraded particles are either embedded in the counterface or set free within the contact zone. All of the samples that have been subjected to microtribometer tests, with the exception of samples 8 and 10, can be considered to have experienced abrasive wear by the sharp conical probe.

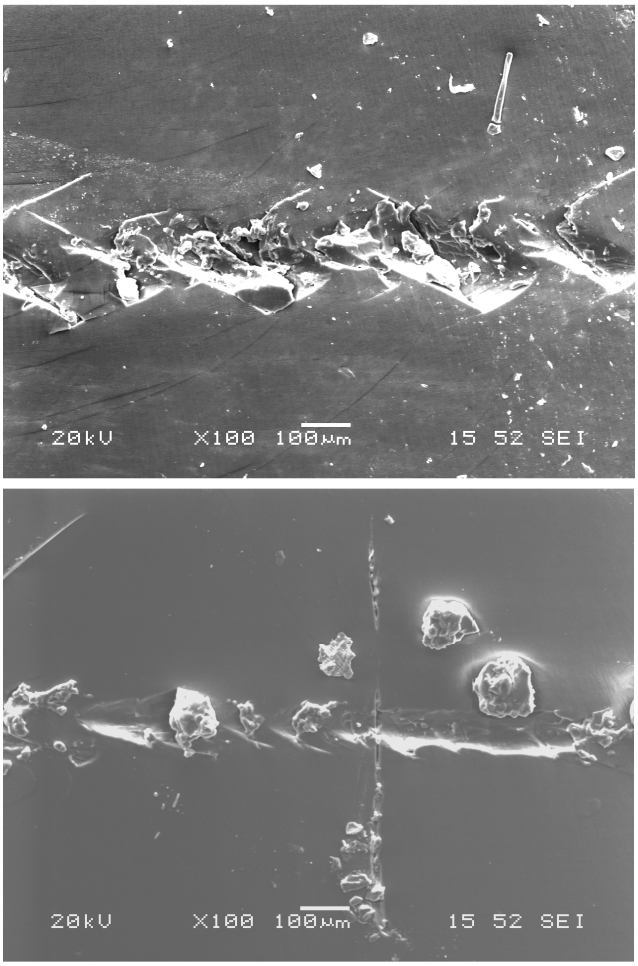

Figure 9. SEM images of sample 4 (top) and sample 9 (bottom) that have been subjected to tests with the reciprocating microtribometer.

Conclusions

CSOY, ST, SG, and HEX or ISO have been polymerized by cationic copolymerization to obtain rubbery materials exhibiting properties similar to commercially available synthetic rubbers. The effects of varying the amounts of ST, diene, and plasticizer have been evaluated using different characterization techniques. It has been determined that increasing the HEX loading decreases the T_g, *E'*, *E"*, and the crosslink density. The tan δ values on the other hand increase with HEX loads. The absence of SG increases the crosslink density, *E'*, and *E"*, but decreases the tan δ, and T_g. Increasing ISO does not seem to have a clear effect on the T_g, tan δ, *E'*, or *E"*. The values here tend to remain relatively constant with only small variations. The crosslink density increases with ISO, but, when SG is absent, the crosslink density doubles. These phenomena do not have a simple explanation, because they are not produced by a single interaction of just one comonomer, but involve a more complex interaction of several parameters that ultimately result in an incremental change in the crosslink density. The thermal properties and soluble portions of these bio-based rubbers do not seem to be affected by the different loads of comonomers, by the nature of the diene used as the crosslinker or by the presence of the plasticizer SG at these particular concentrations. They do, however, affect the tensile characteristics by increasing the Young's modulus and lowering the ultimate strain, when no SG is added. ISO helps to prevent abrasion when compared with the corresponding HEX samples. In some cases, no abrasion is observed for the ISO samples, suggesting that these materials have a performance more like synthetic rubbers than the HEX bio-based rubbers. It is evident that ISO is superior to HEX as an additive for these bio-rubbers. In general, better mechanical and thermal

properties are achieved when ISO is present, instead of HEX, but some improvement in the mechanical properties is necessary to match the properties of commercially available rubbers, especially if the materials are going to be subjected to constant stress. We recommend these rubbers for applications where damping vibrations is important, such as small pieces for car doors or seats, for spacers in paneling, *etc*.

Acknowledgements

The authors would like to thank Ag Environmental Products L.L.C. for the kind donation of the SoyGold® and also the Plant Sciences Institute at Iowa State University for financial support of this project.

References

[1] Yang, S.; Lohnes, R. A.; Kjartanson, B. H. "Mechanical Properties of Shredded Tires," *Geotechnical Testing Journal*, GTJODJ, Vol. 25, No. 1, March 2002, pp. 44-52.

[2] Sombatsompop, N.; Kumnuantip, C. J. Appl. Polym. Sci. 2003, 87, 1723-1731.

[3] Larock, R. C.; Dong, X.; Chung, S.; Reddy, C. K.; Ehlers, L. E. J. Am. Oil Chem. Soc. 2001, 78, 447-453.

[4] Li, F.; Hanson, M. V.; Larock, R. C. Polymer 2001, 42, 1567-1579.

[5] Li, F.; Larock, R. C. J. Appl. Polym. Sci. 2000, 78, 1044-1056.

[6] Li, F.; Larock, R. C. "Synthesis, Properties, and Potential Applications of Novel Thermosetting Biopolymers from Soybean and Other Natural Oils," in: *Natural Fibers, Biopolymers, and Biocomposites,* Mohanty, A.; Misra, M.; Drzal, L., Eds., Taylor & Francis Group, Boca Raton 2005, p. 727.

[7] Li, F.; Larock, R. C. J. Polym. Sci. B: Polym. Phys. 2001, 39, 60-77.

[8] Li, F.; Hanson, M. V.; Larock, R. C. Polymer 2001, 42, 1567-1579.

[9] Di Pierro, P.; Chico, B.; Villalonga, R.; Mariniello, L.; Damiao, A.; Masi, P.; Porta, P. Biomacromolecules 2006, 7, 744-749.

[10] Neto, C. G.; Giacometti, J. A.; Job, A. E.; Ferreira, F. C.; Fonseca, J. L.; Pereira, M. R. Carbohyd. Polym. 2005, 62, 97-103.

[11] Andjelkovic, D. D.; Valverde, M.; Henna, P.; Li, F.; Larock, R. C. Polymer 2005, 46, 9674-9685.

[12] Li, F.; Larock, R. C. J. Polym. Sci. B: Polym. Phys. 2000, 38, 2721-2738.

[13] Li, F.; Larock, R. C. J. Appl. Polym. Sci. 2001, 80, 658-670.

[14] Lu, Y.; Larock, R. C. Biomacromolecules 2006, 7, 2692-2700.

[15] Lu, Y.; Larock, R. C. Biomacromolecules 2007, 8, 3108-3114.

[16] Valverde, M; Andjelkovic, D.; Kundu, P.; Larock, R. C. J. Appl. Polym. Sci. 2008, 107, 423-430.

[17] Kundu, P. P.; Larock, R. C. Biomacromolecules 2005, 6, 797-806.

[18] Henna, P. H.; Larock, R. C. Macromol. Mater. Eng. 2007, 292, 1201-1209.

[19] Mauldin, T. C.; Haman, K.; Sheng, X.; Henna, P.; Larock, R. C.; Kessler, M. R. J. Polym. Sci. Part A 2008, 45, 6851-6860.

[20] Lu, Y.; Larock, R. C. Biomacromolecules 2008, 9, 3332-3340.

[21] Valverde, M.; Jackson, J. M.; Larock, R. C., submitted to *Polymer*.

[22] Andjelkovic, D. D.; Min, B.; Ahn, D.; Larock, R. C. J. Agric. Food Chem. 2006, 54, 9535-9543.

[23] Shaji, J.; Kuruvilla, J.; Sabu, T. Intern. J. Polym. Mater. 2006, 55, 925-945.

[24] Mishra, J.; Chang, Y.; Kim, D. Mater. Lett. 2007, 61, 3551-3554.

[25] Parulekar, Y.; Mohanty, A. Green Chem. 2006, 8, 206-213.

[26] Mohanty, A.;Wu, Q.; Selke, S. International Patent Office, WO 2006/020998 A2.

[27] Bhuyan, S.; Sundararajan, S.; Holden, L. S.; Andjelkovic, D.; Larock, R. C. Wear 2007, 263, 965-973.

[28] Bhuyan, S.; Sundararajan, S.; Andjelkovic, D.; Larock, R. C., submitted to *Wear*.

[29] Check, K. S.; Karuppiah, K.; Sundararajan, S. J. Biomedic. Mater. Res. Part A 2005, 74A, 687-695.

[30] Odian, G. “Principles of Polymerization,” 4th Ed., Wiley-Interscience: New Jersey, 2004, 690.

[31] Sun, X.; Ni, X. J. Appl. Polym. Sci. 2004, 94, 2286-2294.

[32] Flory, P. J. “Principles of Polymer Chemistry,” Cornell University Press: Ithaca, 1953.

[33] Yoon, S.; Jeong, W.; Valverde, M.; Larock, R. C.; Kessler, M. R. “Thermal Analysis of Bio-based Rubber Composites from Plant Oils,” manuscript in preparation.

CHAPTER 5. CASTOR OIL-BASED WATERBORNE POLYURETHANE DISPERSIONS REINFORCED WITH CELLULOSE NANOWHISKERS

A Paper to be Published in Journal of Applied Polymer Science

Marlen Valverde, Yongshang Lu, and Richard C. Larock*

Department of Chemistry, Iowa State University, Ames, Iowa 50011

Abstract

Novel waterborne polyurethane (PU) nanocomposite films containing ~50 wt % of castor oil and various loadings of cellulose nanowhiskers (CNWs) have been synthesized. A comparison of the thermal and mechanical properties generated by incorporation of the nanowhiskers by physical and chemical means is presented. FT-IR spectra and SEM imaging indicate the presence of a high degree of interaction between the nanofiller and the matrix. The T_g and tan δ values for the nanocomposites are generally lower than the values for the pure matrix, while *E'* and *E"* increase from 18 and 13 MPa to 164 and 73 MPa, respectively. The thermal stability increases with addition of the CNWs for all of the films. The Young's modulus more than doubles with up to 10 wt % of the CNWs, the tensile strength increases from 2.1 MPa to 10.3 MPa in the physically incorporated CNWs films and to 15.8 MPa for the chemically incorporated nanocomposites. All of the mechanical effects are more evident in the chemically incorporated CNWs films.

Introduction

Polyurethanes (PUs) are a very important class of polymeric materials that have a wide variety of applications, ranging from adhesives, to clear films, to wood varnishes, to biomedical artifacts, due to their appreciable physical and mechanical properties and good biocompatibility when the appropriate monomers are used.[1,2] The various properties of a PU can be tuned by choosing the correct diisocyanate and polyol comonomers from an extensive list of candidates, and thereby expanding, the range of applications of this class of polymers. Common commercially available PUs have the negative characteristic of containing large amounts of organic solvents and in some cases even free isocyanate molecules that present an environmental and human health problem.[3]

In order to minimize the amount of petroleum-based substances in PUs, increasing efforts have been made to (1) introduce waterborne dispersions, which greatly reduce the volatile organic compounds (VOCs) emitted;[4] (2) use bio-based polyols, such as polycaprolactone, polyalkylene adipate, polylactides, and polyglycolides;[5] and (5) more recently introduce vegetable oil-based hard segment tunable latexes.[6] The preparation of polymers from renewable sources, such as vegetable oil-based materials, is currently receiving increasing attention, because of the economic and environmental advantages.[7-10] In order to use common vegetable oils, like soybean oil, as starting materials for polyurethane synthesis, it is necessary to functionalize them to form polyols.[4-6] Epoxidation and ring opening by acids or alcohols, and ozonolysis are some of the methods used for functionalization of the carbon-carbon double bonds of the triglycerides.[11-15] Castor oil (CO), extracted from the seed of the *Ricinus communis* tree,

contains 90% ricinoleic acid (12-hydroxy-*cis*-9-octadecenoic acid)[16] and it does not need to be chemically modified since it is already a polyol. Thus, castor oil is a cheap, readily available, and biorenewable raw material that is a great alternative for the preparation of bio-based polyurethanes.

Other synthetic approaches to the reduction of harmful petroleum-based substances in PUs or polymeric materials in general that also improve the thermal and mechanical properties of the polymers have involved the introduction of fillers, particularly bio-based fillers.[17,18] Carbohydrates have been used as a biodegradable matrix (starch) or a filler (cellulose) in several high-performance composite materials.[19-23]

When cellulose is treated with a strong acid, it hydrolyzes into microcrystalline cellulose (MCC).[24] The dimensions of the MCC depend on the origin of the cellulose. They can be short (0.1 μm), for cotton and wood cellulose, or long (~10 μm) for tunicates or seaweeds.[25] MCC can be broken down into cellulose nanowhiskers (CNWs) by chemical and mechanical treatments.[26] The use of highly CNWs as a nanofiller leads to mechanical improvements in certain polymers.[27,28] Compared to inorganic fillers, the main advantages of CNWs are their renewable nature, they are the by-product of agricultural activities, low energy consumption, low cost, and high strength and modulus.[22]

In this paper, we introduce CNWs as bio-based nanofillers in combination with CO-based waterborne PU dispersions to improve their thermal and mechanical characteristics and to maximize the content of biorenewable materials in the final products. We also present a comparison of the properties that arise from the different physical and chemical means of incorporating the CNWs into the matrix.

Experimental Section

Materials. Castor oil with an OH number of 163 mg KOH/g, hexamethylenediisocyanate (HDI), dimethylolpropionic acid (DMPA), and *N*,*N*-dimethylacetamide (DMAc) were purchased from Aldrich Chemical and used as received. Triethylamine (TEA), methyl ethyl ketone (MEK), and *N*,*N*-dimethylformamide (DMF) were purchased from Fisher Scientific and used without further purification. Microcrystalline cellulose (MCC) Ceolus ® KG-802 was generously supplied by Asahi Kasei Chemicals Corporation of Tokyo, Japan. This MCC is a commercially available, pharmaceutical grade cellulose used as the starting material for the swelling/separation of the whiskers. The particle sizes of the MCC range between 10 and 15 μm.

Swelling and Separation of the MCC. The MCC was separated into cellulose nanowhiskers (CNWs) following a procedure described by K. Oksman *et. al.* with some minimal modifications.[26] A 20 wt % solution of MCC in DMAc with 0.5 wt % of LiCl as a swelling agent was stirred at 800 rpm for 24 h at 70 ^{o}C; after that, the solution was sonicated in an ultrasonic bath for 3 h periods over 5 d with 24 h intervals between treatments. The resulting CNWs solution was sonicated for 3 h prior to introduction of the PU dispersions.

Synthesis of the CO-PU Dispersions. Two types of CO-based waterborne PU dispersions were synthesized to create a series of nanocomposites by physical incorporation of the filler and chemical incorporation of the nanofiller, the difference in processes been dictated by the precise moment at which the nanofiller is incorporated into the dispersions. For physical incorporation of the CNWs, a large batch of CO-PU

was synthesized in the following manner: CO (45 g), HDI, and DMPA were added to a three-necked round-bottom flask equipped with an overhead stirrer, a condenser and a thermometer. The molar ratio between the NCO groups of the HDI, the OH groups of the CO and the OH groups of the DMPA was 2.0/1.0/1.0. The temperature of the reaction was kept at 78 ^{o}C for 30 min with continuous stirring. At this point, 90 mL of MEK were added to reduce the viscosity of the system. The PU dispersion was allowed to stir for 2 h and then it was cooled down to 40 ^{o} C before the addition of TEA (1.2 equivalents per DMPA). After 1 h of high speed stirring, enough deionized water was added to make a 20 wt % solids dispersion. The high speed stirring was continued for 1 h at room temperature. The MEK was removed under vacuum. The resulting CO-based waterborne PU dispersion was mixed with different amounts of a 20 wt % DMAc solution of CNWs to prepare nanocomposite dispersions of 0.5, 1.0, 1.5, 2.0, 3.0, 5.0, 7.0, and 10.0 wt % CNWs. Each nanocomposite dispersion was sonicated for 2 h and then cast on a clean rectangular glass mold and allowed to dry for 24 h. The resulting films had a mass of around 5 g of solids. For chemical incorporation of the CNWs, CO (15 g), HDI, and DMPA were added to several three-necked round-bottom flasks equipped with an overhead stirrer, a condenser and a thermometer. After 20 min of stirring at 78 ^{o}C, different amounts of the 20 wt % DMAc solution of CNWs were added to the flasks. The molar ratio between the NCO groups of the HDI, the OH groups of the CO and the OH groups of the DMPA was 2.5/1.0/1.0. After 30 more minutes of stirring, 30 mL of MEK were added to reduce the viscosity of each system. From this point forward, the sample preparation was the same as that followed for physical incorporation of the samples. See Scheme 1.

Characterization. The morphology of the CNWs obtained after the sonication process was observed on a transmission electron microscope 200 kV JEOL 1200EX, Japan Electron Optics Laboratory (Peabody, MA). The CNWs solution was diluted in DMAc to 0.2 wt %, a drop of this solution was placed on a carbon film grid and allowed to dry, and then negatively stained with a solution of 1 wt % uranil acetate (UAc) in DI water.

The FT-IR spectra of some films were obtained using a Nicolet 460 FT-IR spectrometer (Madison, WI).

The dynamic mechanical properties of the samples were studied using a model Q800 dynamic mechanical analyzer DMA (TA Instrument) in tensile mode. The rectangular specimens obtained from the dried films had dimensions of 0.5 × 5 × 30 mm ($t \times w \times l$). The temperature range of the analysis was -100 °C to 150 °C at a heating rate of 3 °C/min. All measurements were conducted using an amplitude of 10.0 μm, and a frequency of 1 Hz. The storage and loss moduli and tan δ values were recorded as a function of temperature. The glass transition temperatures (T_g) of the samples were measured from the peaks of the tan δ curves.

Differential scanning calorimetry (DSC) was performed of a thermal analyzer Q20 (TA Instrument). The samples were heated from room temperature to 100 °C at a rate of 10 °C/min to erase all thermal history, and then they were cooled to -70 °C and heated to 150 °C at a rate of 5 °C/min. The glass transition temperature (T_g) was determined from the temperature/heat capacity graph of the second heating scan as the midpoint temperature of the observed secondary transition.

The thermogravimetric analyses were performed on a model Q50 TGA Instrument (TA Instruments). The sample was equilibrated at room temperature and then heated to 700 °C at a heating rate of 20 °C/min in air. The weight loss as a function of temperature was measured.

Extraction analyses were performed on ~1 g samples obtained from the dried films. The samples were weighed before being immersed in DMF at room temperature for 48 h. After this, the samples were dried under vacuum at 80 °C for 24 h and finally weighed again to determine the soluble fraction.

The tensile properties of the films were analyzed using an Instron universal testing machine (model 4502) with a crosshead speed of 50 mm/min. Five rectangular specimens of 80 × 10 mm ($l \times w$) dimensions were tested for each sample composition. The reported values are an average of the five specimens.

The scanning electron microscopy was performed on a variable pressure electron microscope Hitachi S-2460 N (Japan) at an accelerating voltage of 20 kV under a helium atmosphere of 60 Pa to observe the morphology of the gold-coated fractured surfaces of the nanocomposites after the tensile tests.

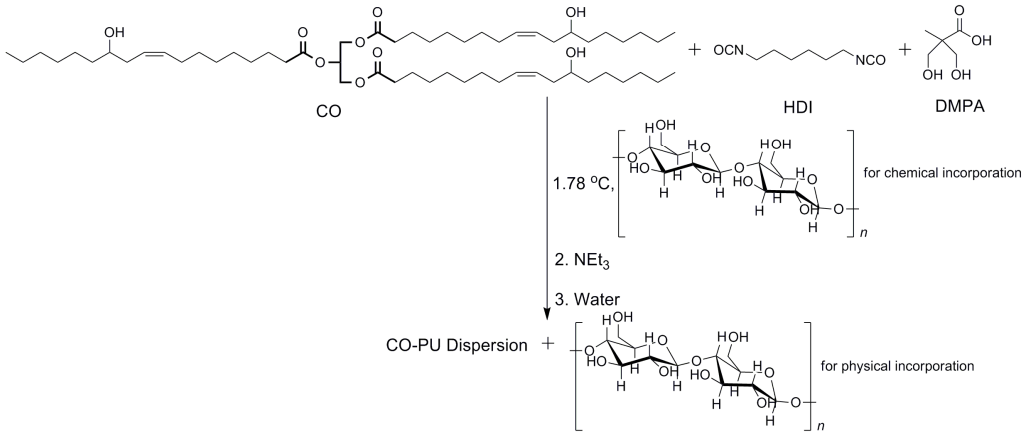

Scheme 1. Synthesis of Castor Oil-Based Waterborne PU Films Containing CNWs.

Results and Discussion

MCC is a highly crystalline material easily obtained from several cellulose sources by acid hydrolysis. The resulting material is an aggregate of a large number of nano-sized crystals called CNWs.[26] The filler-resin interaction in a composite normally increases when the particle size of the filler is small and has a high aspect ratio (*L/d*). In the case of MCC, it is necessary to break down the material into the individual CNWs by a chemical and a mechanical treatment. The process described in the experimental section allows the production of large quantities of CNWs by simple dilution and ultra-sonification. Figure 1 provides a TEM image of the resulting nanowhiskers, which range from 100 to 200 nm in length.

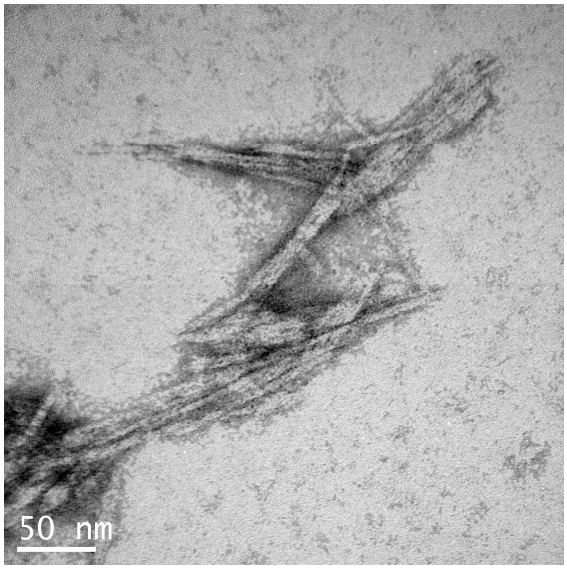

Figure 1. TEM Image of a Diluted Suspension of CNWs in DMAc/LiCl.

Castor oil, on average, has 2.5-2.7 OH groups per triglyceride.[5] These hydroxyl groups are capable of reacting with diisocyanate groups without the need for further chemical modifications to form polyurethanes with a high bio-based content. Under the

reaction conditions used in our polymerizations, the double bonds of the ricinoleic acid and other unsaturated fatty acid chains present in the castor oil are left untouched and remain in the PU films. Many diisocyanate molecules are viable candidates for reaction with the castor oil. In our case, we chose to work with HDI, because we wanted to produce flexible PU films with a high degree of strain in order to be able to clearly observe the effect of adding the nanofiller, which modifies the stretching capability of the materials among other mechanical parameters.[22] DMPA was also incorporated in a molar ratio similar to that of the CO in order to introduce a carboxylic moiety that can react with the TEA to afford PUs, which can be dispersed in water. All PU dispersions for this study were allowed to react for the same amount of time and under the same conditions to minimize the introduction of other variables and to keep the particle size of the PU dispersions constant.

For physical incorporation of the CNWs in the CO-based PUs, the ratio of NCO groups from HDI to the OH groups from CO to the OH groups from DMPA was kept at 2.0/1.0/1.0, but for chemical incorporation of the CNWs, a ratio of 2.5/1.0/1.0 was used, since the excess diisocyanate molecules ought to react with the OH groups of the cellulose and chemically incorporate the whiskers into the PU network.

PU materials are capable of a high degree of hydrogen bonding between the N-H donating groups and the C=O accepting groups. In the case of cellulose-containing films, some degree of hydrogen bonding between the OH groups of the carbohydrate and the C=O of the polyurethane chains is expected. In the past, we have used FT-IR to assess the hydrogen bonding in PUs. Here we also wanted to investigate the interaction between the nanofiller and the matrix. Figure 2 shows the FT-IR spectra of the CO-PU film and 0.5 wt

% CNWs prepared by physical and chemical incorporation of the films. A very distinctive stretching band appears at ~3340 cm^{-1}, which corresponds to a hydrogen-bonded N-H group vibration. A very small shoulder corresponding to the free N-H stretching appears at ~3400-3500 cm^{-1} only for the pure CO-PU, indicating that for the cellulose-containing nanocomposites all of the amide groups are hydrogen bonded. It is assumed that at 0.5 wt % of CNWs the population of OH groups does not generate a band intense enough to be observed. In addition, the sp^2 C-H stretch between ~3000-3200 cm^{-1} is easily observed for the CNW-containing films. In the C=O stretching region, above 1700 cm^{-1} we find peaks originating from free and hydrogen-bonded C=O groups, but, more interestingly, for the CNW-containing films, we also observe peaks between 1650 and 1700 cm^{-1}, which correspond to hydrogen-bonded C=O groups in the highly crystalline regions[29] expected for these nanocomposites. The CO-PU is, on the other hand, an amorphous material indicated by a lack of these highly ordered C=O bands.

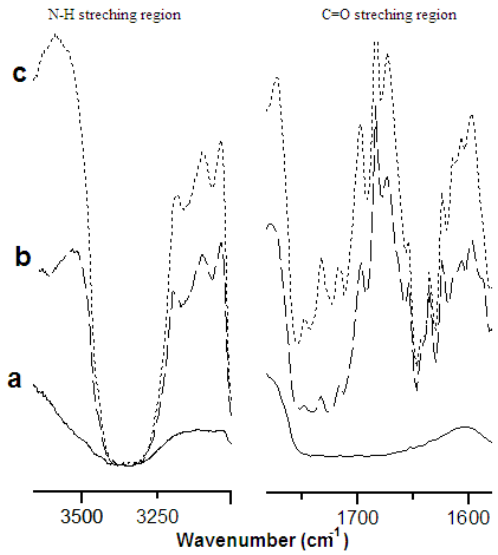

Figure 2. FT-IR Spectra of (a) CO-PU, (b) CO-PU 0.5 wt % CNWs Prepared by Physical Incorporation, and (c) CO-PU 0.5 wt % CNWs Prepared by Chemical Incorporation.

The DSC thermograms of the CO-PU, CNWs and both series of nanocomposites are shown in Figure 3. For the CNWs, it is possible to observe one major endothermic transition between 75-115 ^{o}C, corresponding to the loss of water molecules trapped in the crystalline lattices of the crystallites. No other transitions are observed in the particular temperature range of the analysis. The CO-PU also possesses only one distinctive transition just below 0 ^{o}C. This corresponds to the T_g of the PU chains; see Figure 3(a). For the CO-PU films prepared by physical incorporation of the CNWs, we only observe a T_g transition that slightly, but constantly, decreases as the amount of the CNWs increases in the films [Figure 3(b)]. The same phenomenon is observed for the CO-PU films prepared by chemical incorporation of the CNWs [Figure 3(c)]. In this case, the decrease in T_g is more pronounced. The reason for these decreasing T_g values is the fact that the nanofiller particles interrupt the growth of the PU chains. These smaller chains have higher mobility, which lowers the observed T_g.[30] The chemically-incorporated nanofiller has better interaction with the PU matrix, affecting the chain size in a more direct way, which explains the lower T_g values. The CO-PU films prepared by chemical incorporation of 5.0, 7.0, and 10.0 wt % CNWs do show a very small transition at ~50 ^{o}C, probably corresponding to PU chains with higher incorporation of cellulose that gives them more rigidity.

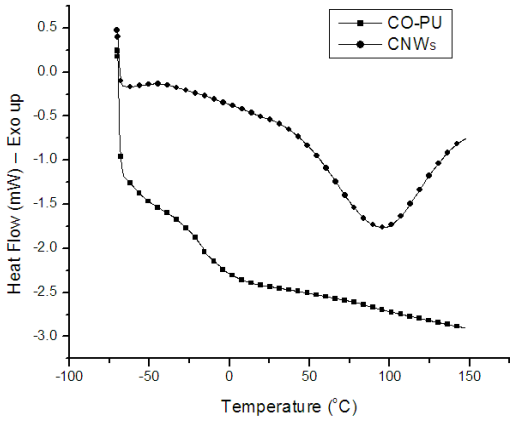

(a) CO-PU and CNWs

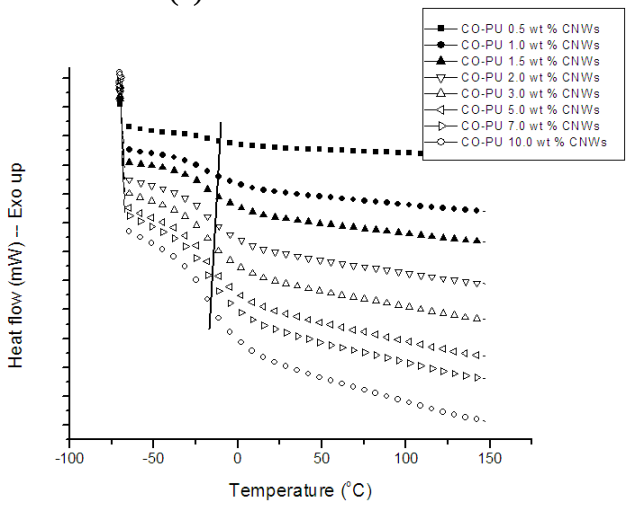

(b) Physical incorporation

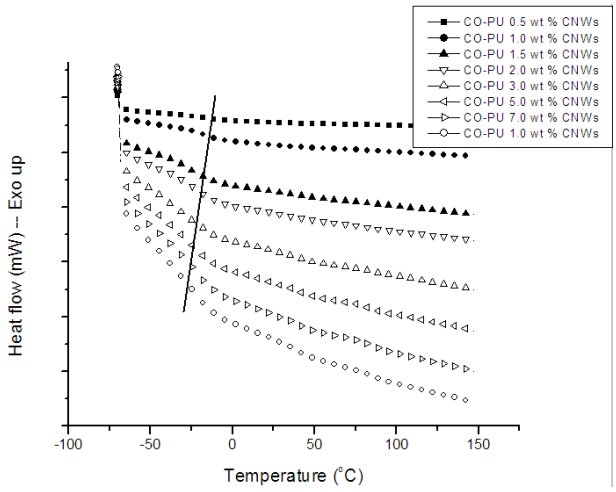

(c) Chemical incorporation

Figure 3. Differential Scanning Calorimetry of the CO-PU, CNWs, and Nanocomposites.

The DMA analyses of the CO-PU and both series of nanocomposites are summarized in Table 1. DMA measures the mechanical stiffness (modulus) and the energy absorption of a material, while applying an oscillating mechanical stress and strain within the linear viscoelastic region. At the T_g, the higher molecular motion within the PU films results in a big decrease in the storage modulus (E') making DMA more sensitive for T_g determinations than DSC. The T_g values here range between 22.6 to 0.4 ^oC. However, in the same way as observed in the DSC analyses, the T_gs of the CNWs-containing films are lower than that of the pure CO-PU. Here, however, we see more variation in the temperatures, which do not exactly follow a clear descending order. This may suggest that interaction between the nanofiller and the matrix is more complex than just the effect on the PU chain length. The degree of hydrogen bonding and filler saturation may also be playing important roles in the resulting T_g values. *E'* and *E"* consistently increase as the amount of nanofiller increases in the PU films [see Figures 4(a) and 4(c)]. This is what is expected when a filler successfully reinforces the originally soft matrix. It is, however, worth noting that the higher *E'* and *E"* values correspond to those of the chemically-incorporated CNWs films, suggesting a better filler-matrix interaction when the filler is chemically bonded to the PU chains. The tan δ values for the PU films prepared by physical incorporation of the CNWs are very similar to the tan δ values of the pure CO-PU, indicating little to no effect of the crystallites in the damping ability of the films [see Figure 4(b)]. For the chemically-incorporated CNWs films, the tan δ values are lower than that of the pure CO-PU. A more pronounced effect is observed for the films with higher loadings of cellulose [Figure 4(d)], further supporting the idea that a better filler-matrix interaction occurs when the CNWs form part of the

polymeric network. PU films with 3.0 and 10.0 wt % chemically-incorporated CNWs were not analyzed by DMA, because they possessed small voids created by bubbles that got trapped in the films during the casting process. Repeated efforts to overcome these problems were unsuccessful.

Table 1. Dynamic Mechanical Analysis of the Castor Oil-Based Waterborne PU Films.

Sample Composition	DMA			
	T_g (°C)	Tan δ	Storage Mod. (MPa)	Loss Mod. (MPa)
CO-PU	22.6	0.73	18	13
CNWs	--	--	--	--
Physical Incorporation				
CO-PU 0.5 wt % CNWs	19.7	0.73	22	16
CO-PU 1.0 wt % CNWs	19.0	0.73	26	19
CO-PU 1.5 wt % CNWs	14.9	0.76	34	25
CO-PU 2.0 wt % CNWs	16.2	0.71	36	25
CO-PU 3.0 wt % CNWs	19.8	0.61	44	27
CO-PU 5.0 wt % CNWs	13.7	0.70	50	34
CO-PU 7.0 wt % CNWs	12.6	0.68	38	26
CO-PU 10.0 wt % CNWs	11.5	0.64	67	43
Chemical Incorporation				
CO-PU 0.5 wt % CNWs	14.7	0.57	34	19
CO-PU 1.0 wt % CNWs	9.9	0.63	60	37
CO-PU 1.5 wt % CNWs	0.4	0.59	95	64
CO-PU 2.0 wt % CNWs	11.4	0.60	49	31
CO-PU 3.0 wt % CNWs	--	--	--	--
CO-PU 5.0 wt % CNWs	4.1	0.40	155	61
CO-PU 7.0 wt % CNWs	6.7	0.45	164	73
CO-PU 10.0 wt % CNWs	--	--	--	--

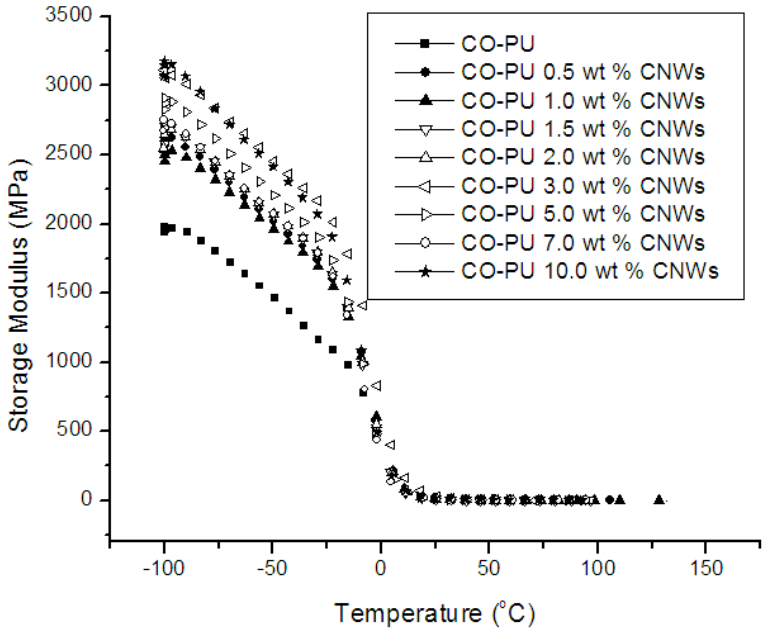

(a) *E'* through physical incorporation

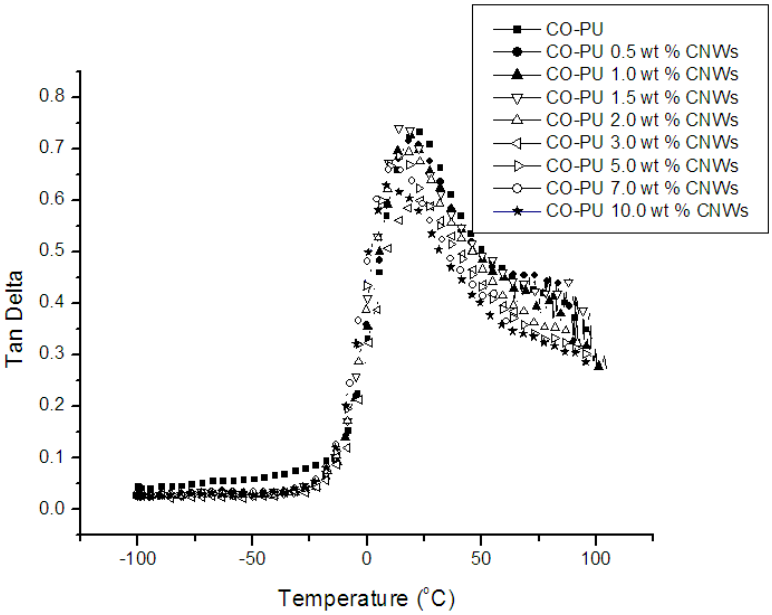

(b)Tan δ through physical incorporation

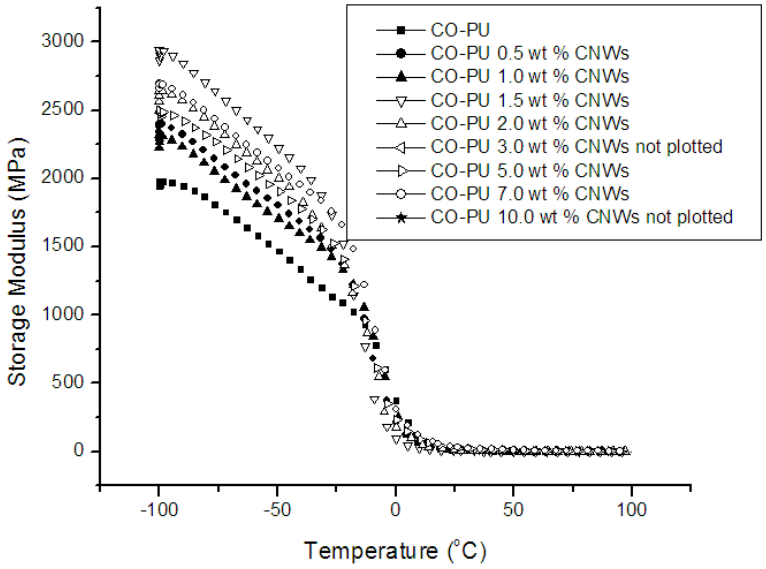

(c) *E'* through chemical incorporation

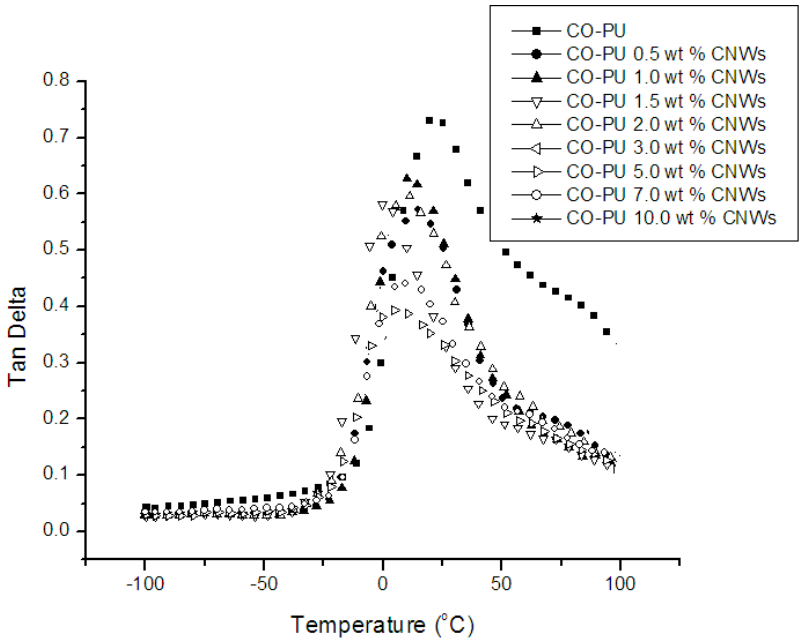

(d) Tan δ through physical incorporation

Figure 4. The Storage Modulus and Tan δ values as a Function of the Temperature for the CO-PU and Nanocomposites.

Table 2 summarizes the TGA and extraction data. For thermal degradation of the PU nanocomposites, it was found that the temperature of 10 % weight loss (T_{10}) for the pure CO-PU is 273 ^{o}C, which corresponds to dissociation of the urethane bonds into amines and olefins or secondary amines and evolution of CO_2. The nanocomposite films exhibit a slightly higher T_{10} value (~280-310 ^{o}C), which suggests that the presence of the CNWs affords some degree of thermal stability to the urethane bonds of the PU matrix, delaying the temperature at which the bonds start to cleave. The temperature of 50 % weight loss (T_{50}) for the CO-PU is 366 ^{o}C, corresponding to degradation of the castor oil triglyceride chains and the bulk of the PU molecules. For the PU nanocomposites, this temperature is again higher, ranging from 376 to 389 ^{o}C, because of the thermal stability afforded by the presence of the CNWs. In addition to degradation of the triglyceride and PU molecules in the nanocomposites, the CNWs also exhibit a 50% weight loss around the above mentioned temperatures (375 ^{o}C). The CO-PU and all of the nanocomposites exhibit two major degradation events that give rise to two distinct temperatures of maximum degradation (T_{max}). The first T_{max} (352-382 ^{o}C) corresponds to degradation of the CNWs, triglyceride, and PU molecules as explained above. The second T_{max} represents the degradation of higher molecular weight-crosslinked PU chains. The CO acts as a crosslinking agent as most of its triglyceride molecules possess two or three OH groups (~ 2.7 OH groups). Due to the high bio-based content of these materials, after their thermo-oxidative degradation around 700 ^{o}C, all samples lose 100% of their original mass, leaving no char behind [see Figure 5].

The extraction analysis of these CNWs-reinforced PU films provides further evidence of the generation of shorter PU chains in the presence of crystallites

(interrupting chain growth) as the soluble portions of the nanocomposites prepared by physical incorporation of the CNWs are significantly higher. For the chemically-incorporated CNWs films, it appears that along with the generation of shorter PU chains, the cellulose particles chemically bond to the chains, making them insoluble in DMF and thus creating a stronger opposite effect, which decreases the soluble portion of the materials.

Table 2. Thermogravimetric and Soxhlet Extraction Analysis of the Castor Oil-Based Waterborne PU Films.

	TGA			Extraction Analysis	
Sample	T_{10} (°C)	T_{50} (°C)	T_{max} (°C)	**Sol (%)**	**Insol (%)**
CO-PU	273	366	352/487	4.9	95.1
CNWs	345	375	377	--	--
Physical Incorporation					
CO-PU 0.5 wt % CNWs	292	377	382/507	7.7	92.3
CO-PU 1.0 wt % CNWs	292	380	374/503	15.0	85.0
CO-PU 1.5 wt % CNWs	287	373	376/510	13.8	86.2
CO-PU 2.0 wt % CNWs	283	377	379/504	11.3	88.7
CO-PU 3.0 wt % CNWs	281	379	379/514	10.5	89.5
CO-PU 5.0 wt % CNWs	279	376	368/514	9.8	90.2
CO-PU 7.0 wt % CNWs	279	381	374/506	8.8	91.2
CO-PU 10.0 wt % CNWs	279	388	363/513	8.0	92.0
Chemical Incorporation					
CO-PU 0.5 wt % CNWs	310	384	381/487	7.4	92.6
CO-PU 1.0 wt % CNWs	305	386	378/509	7.2	92.8
CO-PU 1.5 wt % CNWs	287	379	376/506	6.0	94.0
CO-PU 2.0 wt % CNWs	299	387	377/503	5.7	94.3
CO-PU 3.0 wt % CNWs	279	382	372/506	5.2	94.8
CO-PU 5.0 wt % CNWs	289	385	369/511	4.5	95.5
CO-PU 7.0 wt % CNWs	291	389	369/507	2.9	97.1
CO-PU 10.0 wt % CNWs	281	386	372/499	2.9	97.1

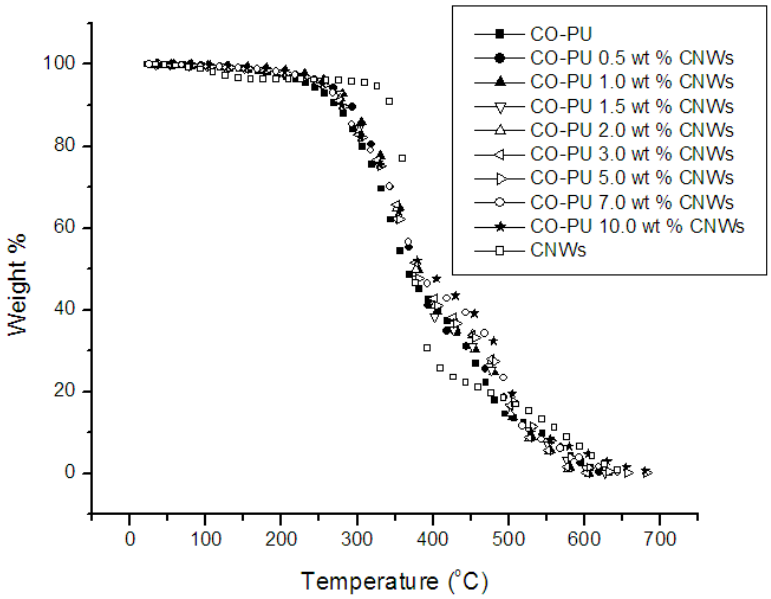

(a) Physical incorporation

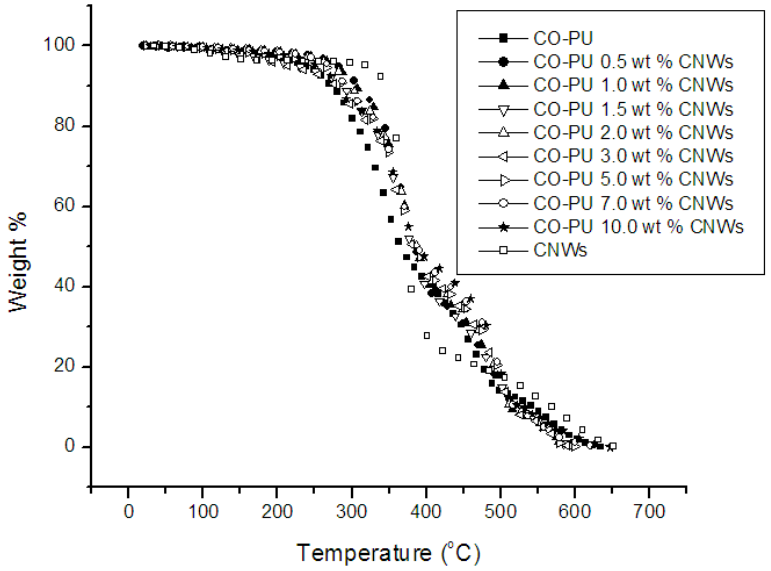

(b) Chemical incorporation

Figure 5. Thermogravimetric Analyses of the CO-PU, CNWs, and Nanocomposites.

Table 3 summarizes the mechanical properties observed during tensile analysis of the CO-based waterborne PU films. In general, the Young's modulus and the tensile strength of the CNWs-containing films increase steadily from the original values

exhibited by the pure CO-PU. This is in agreement with what is expected from a true reinforcing nanofiller. The modulus increases to 2.5 times that of the original value of the CO-PU when 7.0 to 10.0 wt % of CNWs are incorporated. Both the physically- and chemically-incorporated CNWs films reach a maximum around the same value (~80 MPa). The tensile strength increases to higher values for the chemically-incorporated CNWs films, which indicates a better reinforcing action for the chemically-bonded whiskers. Failure strain in tensile mode is a parameter that best describes the ability of films to stretch. A decrease in values, like the one observed for the CNWs-containing films, indicates an increasing brittleness of the materials as the load of the nanofiller increases. The effect is higher for the chemically-incorporated CNW films as the values fall from 493% to 91% with 7.0 wt % CNWs. During the tensile tests, the specimens from the physically incorporated CNW films exhibit necking before snapping. The samples from the chemically-incorporated CNW films do not show a similar trend, corroborating their brittle nature. The stress-strain curves of the PU films are shown in Figure 6. The toughness of the materials was calculated from the area under each individual curve. It is defined as the resistance to break under applied stress and normally decreases for brittle materials.[31] In the case of these CO-based waterborne PU films, the opposite trend is observed, the more brittle films exhibit the higher toughness values. One reason for this unexpected behavior might be an improved interaction between the filler and the matrix, making these materials more resistant to fracture with higher loads of nanofiller.

Table 3. Tensile Analysis of the Castor Oil-Based Waterborne PU Films.

Sample	Modulus (MPa)	Toughness (MPa)	Strength (MPa)	Failure Strain (%)
CO-PU	32.4 ± 0.2	4.3 ± 0.5	2.1 ± 0.1	493 ± 31
Physical Incorporation				
CO-PU 0.5 wt % CNWs	57.8 ± 0.8	5.6 ± 0.1	2.4 ± 0.3	434 ± 25
CO-PU 1.0 wt % CNWs	60.5 ± 0.3	6.4 ± 0.7	2.9 ± 0.4	412 ± 33
CO-PU 1.5 wt % CNWs	54.7 ± 0.5	8.4 ± 0.3	3.5 ± 0.6	396 ± 42
CO-PU 2.0 wt % CNWs	64.2 ± 0.4	8.4 ± 0.6	4.1 ± 0.2	376 ± 24
CO-PU 3.0 wt % CNWs	63.1 ± 0.7	11.0 ± 0.5	5.0 ± 0.7	349 ± 36
CO-PU 5.0 wt % CNWs	79.7 ± 0.9	14.0 ± 0.2	7.0 ± 0.5	324 ± 18
CO-PU 7.0 wt % CNWs	79.6 ± 0.3	17.5 ± 0.7	8.5 ± 0.6	296 ± 21
CO-PU 10.0 wt % CNWs	82.5 ± 0.3	21.1 ± 0.1	10.1 ± 0.2	260 ± 27
Chemical Incorporation				
CO-PU 0.5 wt % CNWs	43.9 ± 0.6	3.6 ± 0.4	2.5 ± 0.2	208 ± 13
CO-PU 1.0 wt % CNWs	50.1 ± 0.3	4.2 ± 0.2	3.4 ± 0.4	183 ± 32
CO-PU 1.5 wt % CNWs	61.2 ± 0.4	5.0 ± 0.3	4.6 ± 0.6	165 ± 24
CO-PU 2.0 wt % CNWs	62.4 ± 0.2	5.1 ± 0.8	5.2 ± 0.4	149 ± 15
CO-PU 3.0 wt % CNWs	--	--	--	--
CO-PU 5.0 wt % CNWs	85.1 ± 0.2	8.6 ± 0.7	10.3 ± 0.3	111 ± 11
CO-PU 7.0 wt % CNWs	85.1 ± 0.4	10.1 ± 0.3	15.8 ± 0.2	91 ± 8
CO-PU 10.0 wt % CNWs	--	--	--	--

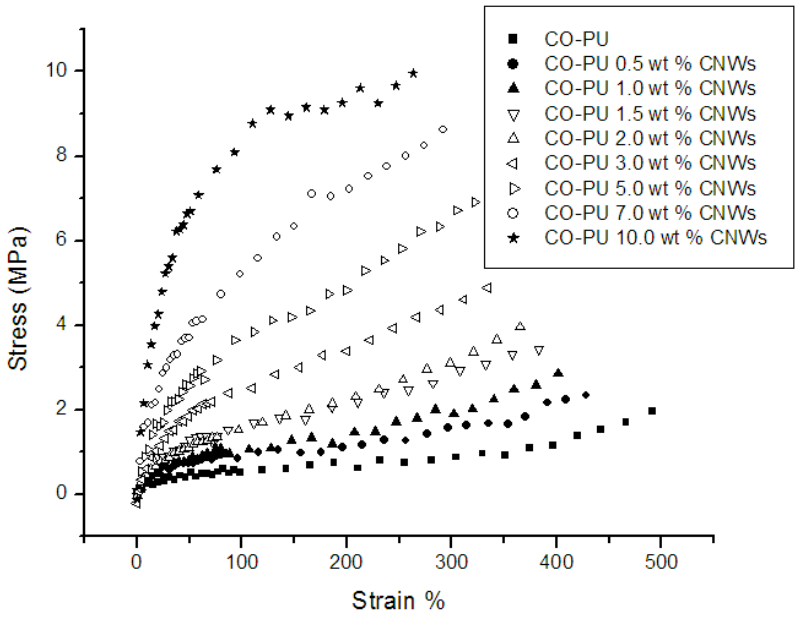

(a) Physical-incorporation

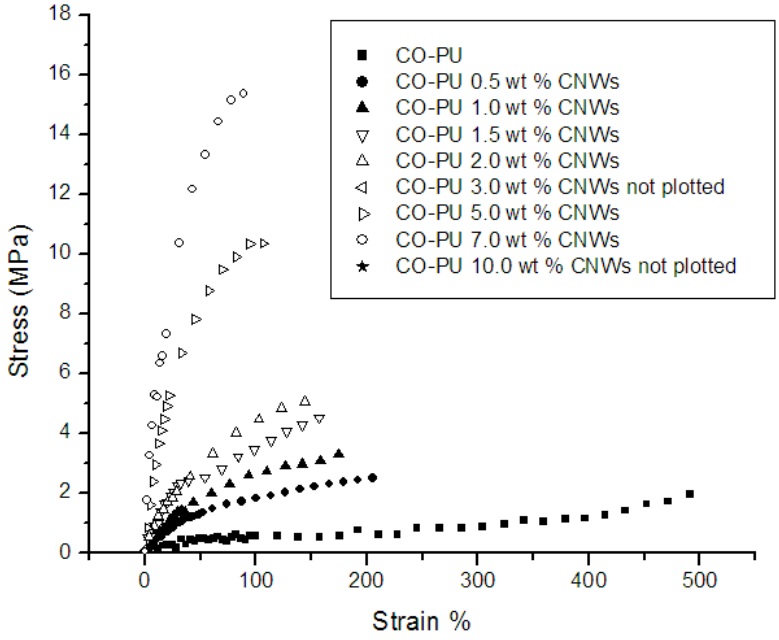

(b) Chemical-incorporation

Figure 6. Tensile Analyses of the CO-PU and Nanocomposite Films.

Figure 7 illustrates the SEM images of the fractured surfaces after the tensile tests of the CO-PU and nanocomposites with low (0.5 wt %) and high (7.0 wt %) loads of CNWs for both physical and chemical incorporations of the CNWs. The CO-PU [Figure

7(a)] surface exhibits a very “clean” fracture with just small debris particles in accordance with what is expected of a pure resin sample. For the CO-PU with 0.5 wt % CNWs prepared by physical incorporation, fewer, but larger, formations appear on the fractured surface, suggesting the presence of an interaction between the matrix and the filler. This interaction is noticeably enhanced in the CO-PU with 0.5 wt % CNWs prepared by chemical incorporation [Figure 7(c)], which shows a rough surface with spherical particles, a possible product of the growth of PU chains around the CNWs. As the amount of the nanofiller increases in the physically-incorporated films, one observes that the fractured surface becomes more complex with larger debris, but still with somewhat smooth areas [see Figure 7(d)]. For the CO-PU with 7.0 wt % CNWs prepared by chemical incorporation [Figure 7 (e)], the fractured surface clearly indicates a high degree of filler-matrix interaction, as it is rough and contains many uneven areas. These images help corroborate the significant mechanical differences observed between physical and chemical incorporation of the CNWs into the CO-based waterborne PUs.

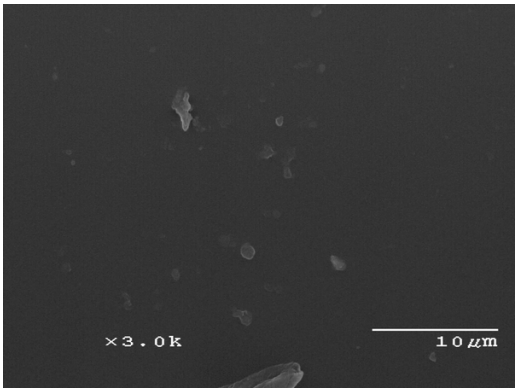

(a) CO-PU

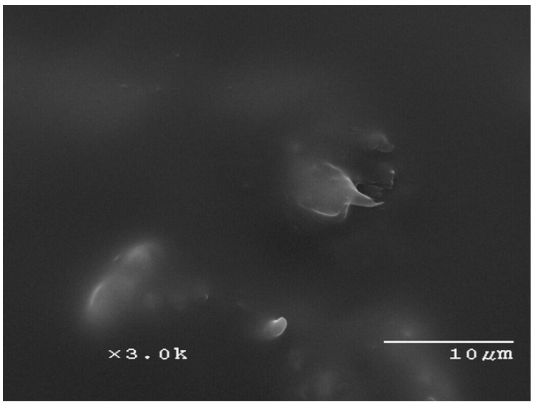

(b) CO-PU with 0.5 wt % CNWs prepared by physical incorporation

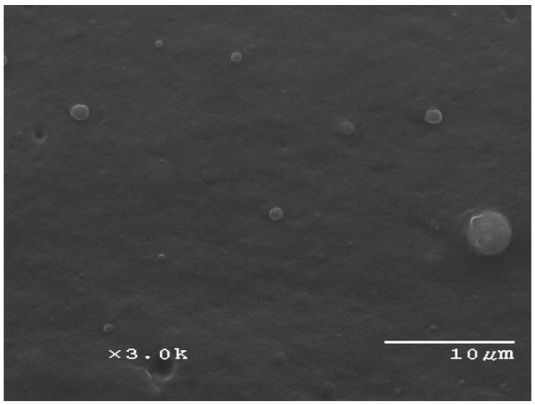

(c) CO-PU with 0.5 wt % CNWs prepared by chemical incorporation

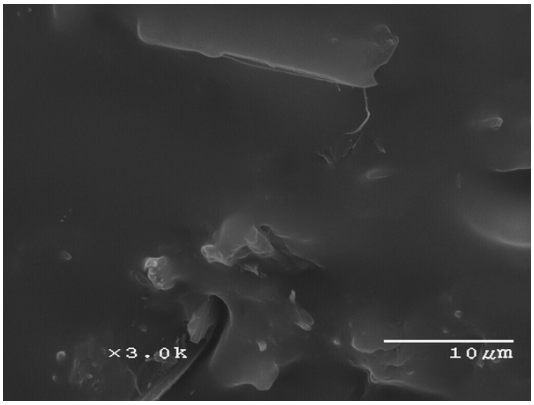

(d) CO-PU with 7.0 wt % CNWs prepared by physical incorporation

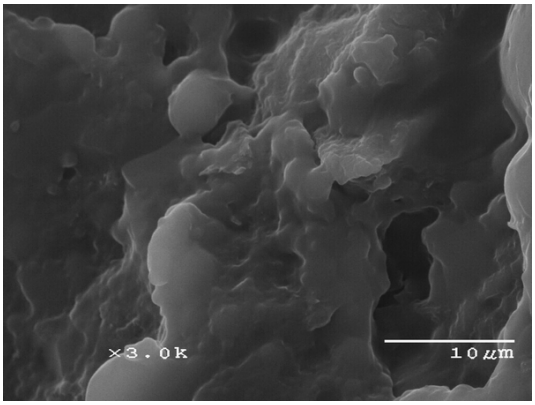

(e) CO-PU with 7.0 wt % CNWs prepared by chemical incorporation

Figure 7. SEM Micrographs of the Fractured Surfaces of the Films After the Tensile Analysis.

Conclusions

A novel waterborne PU film containing ~50 wt % of castor oil has been synthesized by reacting the oil with a flexible diisocyanate, HDI. The resulting transparent film exhibits a rather low tensile strength and high elongation at break (493 ± 31%). It has been especially engineered so as to be modified by the addition of CNWs. Two series of CO-based waterborne PU nanocomposites reinforced by chemical and physical means with CNWs have been synthesized. These series have been compared to see the effect of the presence of the crystallites in the matrix. In one case, a simple physical interaction between the matrix and the filler exists, and in the other case, chemical bonds are formed between them, allowing the OH groups of the cellulose to react with an excess of the HDI. For both systems, the CNWs, when blended, from a 20 wt % solution in DMAc are compatible with the CO-based waterborne PU in loads of up to 10.0 wt %. FT-IR spectra show the existence of C=O hydrogen bonding in the urethane groups in highly crystalline regions.

The effect of varying the amount of CNWs and the method of incorporation of the CNWs have been evaluated using different characterization techniques. It has been determined that increasing the CNWs load decreases the T_g and tan δ values, while *E'* and *E"* tend to increase for the two series of nanocomposites. The changes are more evident in the chemically-incorporated CNWs series of films as the parameters vary greatly with small changes in the CNWs concentration. DSC analysis confirms the tendency of the T_g to decrease with a higher load of CNWs, presumably by promoting the formation of shorter PU chains during polymerization.

The CO-based PU nanocomposites benefit thermally from the addition of CNWs as observed in the thermal degradation curves (Figure 5). In all cases, the T_{10}, T_{50}, and T_{max} values increase with the CNWs load due to the highly crystalline framework of the cellulose whiskers. The thermal improvement, however, is limited by cellulose's own degradation at ~ 380 ^{o}C.

The mechanical properties of these nanocomposites are also positively impacted by the presence of the CNWs in the PU matrix. Again, chemical incorporation enhances the parameters with fewer CNWs. The Young's modulus, tensile strength, and toughness increase significantly, converting the original soft and flexible films into tough and somewhat brittle white nanocomposites.

The favorable interaction of the CNWs and the PU matrix is captured in the SEM images of Figure 7. There is evidence of increasing filler-matrix interaction as the fractured surfaces present a more complex rupture with increasing loads of CNWs, especially for the films with chemically-incorporated crystallites.

Some interesting possible uses of these novel bio-based nanocomposites are coating applications where biodegradability is necessary, adhesives for biomedical uses, "green" paints, *etc*.

Acnowledgements

The authors would like to thank Professor Michael Kessler of the Department of Material Sciences and Engineering at Iowa State University for the use of his thermo-mechanical testing instrument laboratory, Mrs. Tracey M. Pepper of the Microscopy and NanoImaging Facility at Iowa State University for her kind assistance with the TEM

analysis, and Mr. Warren Straszheim of the Materials Analysis Research Laboratory at Iowa State University for assistance with the SEM analysis.

References

1. Lelah, M. D.; Cooper, S. L. Polyurethanes in Medicine; CRC Press: Boca Raton, 1986; p 4.

2. Planck, H.; Syre, I.; Dauner, M.; Egbers, G. Polyurethanes in Biomedical Engineering; Elsevier Science: Amsterdam, 1987; p 6.

3. Kim, B. S.; Kim, B. K. J. Appl. Polym. Sci. 2005, 97, 196.

4. Lu, Y.; Larock, R. C. Biomacromolecules 2007, 8, 3108.

5. Yeganeh, H.; Hojati-Talemi, P. Polym. Deg. Stab. 2007, 92, 480.

6. Lu, Y.; Larock, R. C. Biomacromolecules 2008, 9, 3332.

7. Valverde, M.; Andjelkovic, D.; Kundu, P.; Larock, R. C. J. Appl. Polym. Sci. 2008, 107, 423.

8. Uyama, H.; Kuwabara, M.; Tsujimoto, T.; Kobayashi, S. Biomacromolecules 2003, 4, 211.

9. Tsujimoto, T.; Uyama, H.; Kobayashi, S. Macromolecules 2004, 37, 1777.

10. Biermann, U.; Friedt, W.; Lang, S.; Luhs, W.; Machmuller, G.; Metzger, J.; Angew. Chem. Int. Ed. 2000, 39, 2206.

11. Hill, K. Pure Appl. Chem. 2000, 72, 1255.

12. Petrovic, Z. S.; Zhang, W.; Javni, I. Biomacromolecules 2005, 6, 713.

13. Okieimen, F. E.; Pavithran, C.; Bakare, I. O. Eur. J. Lipid. Sci. Technol. 2005, 107, 330.

14. Eren, T.; Kusefoglu, S. H. J. Appl. Polym. Sci. 2004, 91, 4037.

15. Petrovic, Z. S.; Guo, A.; Zhang, W. J. Polym. Sci. Part A - Polym. Chem. 2000, 38, 4062.

16. Baber, T. M.; Vu, D. T.; Lira, C. T. J. Chem. Eng. Data 2002, 47, 1502.
17. Quirino, R.; Larock, R. C. J. Appl. Polym. Sci. 2009, 112, 2033.

18. Pfister, D. P.; Baker, J. R.; Henna, P. H.; Lu, Y.; Larock, R. C. J. Appl. Polym. Sci. 2008, 108, 3618.

19. Alvarez, V.; Vazquez, A.; Bernal, C. J. Compos. Mater. 2006, 40, 21.

20. Averous, L.; Fringant, C.; Moro, L. Polymer 2001, 42, 6565.

21. Nattakan, S.; Pitt, S.; Ratana, R. Carbohydr. Polym. 2004, 58, 53.

22. Samir, M. A. S. A.; Alloin, F.; Dufresne, A. Biomacromolecules 2005, 6, 612.

23. Dufresne, A. J. Nanosci. Nanotechnol. 2006, 6, 322.

24. Battista, O. A.; Coppick, S.; Howsmon, J. A.; Morehead, F. F.; Sisson, W. A. Ind. Eng. Chem. 1956, 48, 333.

25. Chanzy, H. In Cellulose Sources and Exploitation; Kennedy, J. F.; Phillips, G. O.; Williams, P. A., Eds.; Ellis Horwwod: New York, 1990, p 3.

26. Oksman, K.; Mathew, A. P.; Bondeson, I.; Kvien, I. Comp. Sci. Tech. 2006, 66, 2776.

27. Dufresne, A.; Kellerhals, M. B.; Witholt, B. Macromolecules 1999, 32, 7396.

28. Grunert, M.; Winter, W. T. J. Polym. Environ. 2002, 10, 27.

29. Pollack, S. K.; Shen, D. Y.; Hsu, S. L.; Wang, Q.; Stidham, H. D. Macromolecules 1989, 22, 551.

30. Wang, Y.; Cao, X.; Zhang, L. Macromol. Biosci. 2006, 6, 524.

31. Rosen, S. Fundamental Principles of Polymeric Materials 2nd Ed.; Wiley-Interscience: New York, 1993; p 310.

CHAPTER 6. GENERAL CONCLUSIONS AND OUTLOOK

This dissertation is a compilation of six chapters dedicated to the exploration of a branch of green chemistry that involves the development of bio-based polymeric materials that will hopefully replace the harmful petroleum-based materials that we use nowadays.

Chapter 1 of this dissertation gives a general introduction together with a brief explanation of the synthetic chemistry behind vegetable oil-based polymeric materials to give the reader a guide as to what the thesis is about and its organization. The second chapter presents a series of interesting new bio-based hard plastics prepared from CLS, AN, and DCP or DVB via free radical polymerization. It was found that the chemical incorporation of the CLS oil into the polymeric network reaches almost 100% when the oil content is 40-65 wt %, particularly for the DCP-containing samples. Lower percentages of oil incorporation into the network are achieved when the oil content nears 85 wt %. Incorporation of the DCP comonomer results in higher tan delta values, when compared to the DVB thermosets, making these materials more promising for applications involving the damping of vibrations. One reason for this result could be that DCP-containing samples have higher chemical incorporation of the CLS oil, which, as stated before, improves vibrational damping, since the longer triglyceride molecules assist the polymeric network in the dissipation of vibrational energy as heat throughout the material. This greater incorporation of long olefinic molecules apparently is not enough to also dramatically affect the T_g values in these samples, as the DVB and DCP

comonomers do not have much influence on the behavior of the T_g's, when comparing the same sample compositions.

The third chapter of this thesis describes the preparation of highly bio-based rubbery materials. All of the samples prepared appear promising from an environmental point of view, since only 1 wt % of the entire composition, the free radical initiatior, is petroleum-based. For the synthesis of these materials, two readily available, bio-renewable vegetable oils were chosen. Tung oil is naturally conjugated and was used without any chemical modification, as it is already a reactive enough vegetable oil under free radical polymerization conditions. Ebecryl® is a soybean oil-based acrylated oil, which has enhanced reactivity when compared with regular soybean oil. These two oils polymerize to form viable rubbery yellow materials without the addition of petroleum-based comonomers, plasticizers, and/or crosslinkers. Chemical incorporation of the oils varies from 6 to 50 wt % as revealed by extraction analyses; the higher percentages of soluble materials correspond to higher amounts of tung oil in the original composition. The unreacted tung oil acts as a plasticizer, increasing the tan delta values, and decreasing the T_gs from ~27 ^{o}C to -25 ^{o}C, providing a wide range of temperatures where these materials can be used to dampen vibrations.

Chapter 4 reports the chemical synthesis and the thermal and mechanical characterization of a series of bio-based rubbers prepared by the cationic polymerization of CSOY, ST, SG (a type of biodiesel), and one of two dienes, HEX and ISO. The main focus of this chapter was to study the effect of varying the type and the amount of the diene, whose main task is to function as a crosslinker in the bio-based rubbers. The materials generated under the chosen experimental conditions are black, soft but tough,

and rather rubbery. It has been determined that increasing the HEX load decreases the T_g, *E'*, *E"*, and the crosslink densities, but the tan δ values increase. Increasing the ISO content does not seem to have a clear effect on the T_g, tan δ, *E'*, or *E"* values. The values here tend to remain relatively constant with only small variations. The crosslink density increases with the ISO content, but, when SG is absent, the crosslink density doubles. It looks like the interaction of the plasticizer SG with the rest of the comonomers is relatively complicated, because, in addition to modifying the T_g and tan δ, it also improves the crosslink density, which are opposite effects. The thermal properties and soluble portions of these bio-based rubbers do not seem to be affected by the different loads of comonomers, by the nature of the diene used or by the presence of the plasticizer SG. However, these variables affect the tensile characteristics by increasing the Young's modulus and lowering the strain, when no SG is added. In this chapter, we study the abrasion characteristics of these materials, since they represent possible substitutes for synthetic rubbers. ISO prevents abrasion much better than the corresponding HEX samples to the point of exhibiting zero wear damage after analysis. In general, we conclude that better mechanical and thermal properties are achieved when ISO is used, instead of HEX, but some improvement in the mechanical properties is necessary to match the properties of synthetic rubbers, especially if the materials are going to be subjected to constant stress. We recommend these rubbers for applications, such as small pieces for car doors or seats, for spacers in paneling, *etc*.

Lastly, Chapter 5 describes some novel waterborne PU films containing 50 wt % of castor oil (CO) and the flexible diisocyanate HDI especially engineered to exhibit rather low tensile strength and a high elongation at break to be later modified by the

addition of CNWs. Two series of CO-based waterborne PU nanocomposites reinforced with CNWs have been synthesized. Two ways to incorporate the CNWs were compared to see the effect of the presence of the crystallites in the matrix, in one case having just a physical interaction between the matrix and the filler, and, in the other case, having chemical bonds between them, allowing the OH groups of the cellulose to react with an excess of HDI. CNWs are compatible with the CO-based waterborne PU in loads of up to 10 wt %. We are able to identify the existence of hydrogen bonding between the matrix and the CNWs as the FT-IR spectra shows the C=O bonds of the urethane groups involved in hydrogen bonding in highly crystalline regions. In general, the addition of CNWs to the CO-based PU films increases the thermal and mechanical properties of the materials, making them potentially more useful industrially. In all cases, chemical incorporation proved to generate the largest positive effects with the least amount of CNWs, indicating also a possible economical advantage. Interesting possible uses of these novel bio-based nanocomposites are (1) coating applications where biodegradability is necessary, (2) adhesives for biomedical uses, (3) “green” paints, *etc*.

As a general conclusion, I would like to add that the main idea behind the design of all of the materials here presented and examined is to prove that it is possible to produce highly bio-based materials that have good chances of becoming viable substitutes for the petroleum-based materials we all know and use daily. It was my main goal to screen several polymerization techniques, vegetable oils, and fillers that ultimately could give a wide range of bio-plastic materials that will hopefully have some useful applications or that at least will serve as an inspiration to future researchers in the area of bio-renewables. Reducing the need for environmentally dangerous substances by

proposing novel feedstocks and polymerization routes was the inspiration for my research.

ACKNOWLEDGEMENTS

I would like to take the opportunity to thank all of the people who at some point helped me by providing valuable conversations from which many of my research ideas flourished. Particularly, I would like to thank Dr. Richard C. Larock for allowing me to be part of his research group, for trusting in me, and for his guidance throughout these years. Many thanks to Dr. Michael Kessler for allowing me the use of his polymer characterization laboratory, to Dr. Yongshang Lu, Dr. Dejan Andjelkovic, Dr. Phillip Henna, Dr. Wonje Jeon, Dan Pfister, Rafael Quirino, and Ying Xia, for their valuable chemical advice and time spent in long discussions about “green” polymers. I also want to thank the rest of the Larock research group members, past and present, for all the useful conversations about organic chemistry. Lastly, I want to thank my dad Federico, my mom Marlen, my brother Federico, and my boyfriend Aurelio for their unconditional love and support, and for giving me good examples of how to achieve my biggest goals, all in the name of science.